Deliverable 3

Testing Protocol and Material Specifications for Basalt Fiber Reinforced Polymer Bars

Contract Number BE694
FSU Project ID: 042878

Submitted to:

Florida Department of Transportation
Research Center
605 Suwannee Street
Tallahassee, Florida 32399-0450

Chase C. Knight, Ph.D
Project Manager
FDOT State Materials Office

Prepared by:

Raphael Kampmann, Ph.D.
Principal Investigator
Youneng Tang, Ph.D.
Co-Principal Investigator
Srichand Telikapalli
Graduate Research Assistant
Sarajeen Saima Hoque
Graduate Research Assistant

FAMU-FSU College of Engineering
Department of Civil and Environmental Engineering
2525 Pottsdamer Street
Tallahassee, FL 32310

04/15/2019

Contents

Chapter 1

Introduction

This deliverable describes the research methodology and lists all experiments that will be conducted on BFRP rebar constituent materials and BFRP rebar products. Several physical, mechanical, and chemical tests will be executed for each rebar sample, raw material, and exposure solution, both before and after exposure to various combinations of saline and alkaline environments. Accordingly, this deliverable focuses on three major aspects: 1) the general experimental concept, 2) the characterization of exposure solutions, and 3) the characterization of BFRP rebar specimens.

1.1 Experimental Concept

This research targets longterm chemical durability of raw and composite materials for the production of basalt fiber reinforced polymer (BFRP) reinforcing bars (rebars). For historic reasons, basalt fibers and their composite materials are lacking behind in the US market. To safely use these materials in civil engineering structures, standardized raw materials and final composite product would be preferable. However, at this stage, standardized FRP rebars seem to be a concept of the future and it is currently more suitable to define minimum acceptance criteria, such that suitable FRP rebar products meet certain performance standards. Accordingly, this research aims to evaluate relevant materials to define the requirements for a safe use of basalt FRP rebars in future civil projects.

Specifically, naked (un-sized) basalt fibers, sized basalt fibers, and resins (epoxy or polyester) from three different sources were obtained as well as final BFRP rebar products, in the two most common sizes (# 3 and # 5), from three different manufacturers. To define the material properties and limit states of the materials, raw and composite materials were exposed to various combinations of saline and alkaline environments conditioned at 60 °C for 300 d and 600 d. Though FRP rebars are typically resistant to harsh environments, BFRP rebars may be susceptible to degradation in harsh environments, depending on the raw materials and the production quality. To study this degradation process, it is important to evaluate the properties of raw materials exposed to harsh environments at accelerated temperatures. Figure 1.1 depicts the various combinations of exposure conditions, which were designed for a systematic variation of alkalinity and salinity. In the test matrix, solid (gray filled) squares signify that the BFRP rebar samples exposed to these environments were tested for mechanical strength, while hollow squares identify the exposure conditions from which raw material samples were drawn for chemical analyses. Finally, the hollow circles (all columns and all rows) identify the chemical environments for which the exposure solutions were examined to measure mass transfers and chemical effects between the raw material component or BFRP rebars and the storage solutions. As seen in the figure, the salinity of the exposure solutions ranged from 0 $\mathrm{mgCl^-/L}$ (deionized water), to 200 $\mathrm{mgCl^-/L}$ (fresh water), and 20 000 $\mathrm{mgCl^-/L}$ (synthetic and real seawater), while the range of pH values

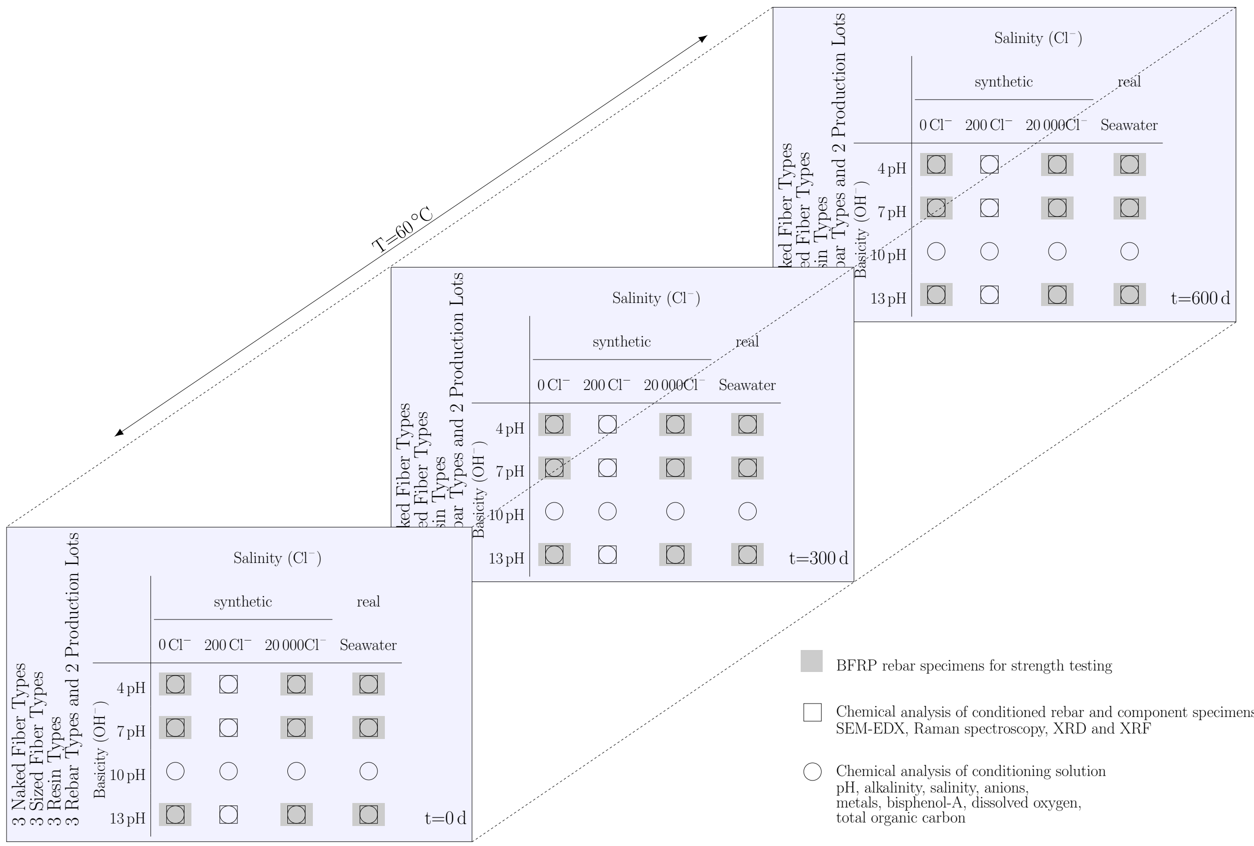

Figure 1.1: Test concept for chemical exposure

varied from 4 pH (acidic solution) to 13 pH (highly caustic solution). These exposure solutions were developed synthetically to eliminate potential contamination and to precisely study the degradation caused by the main factors. However, for a real world comparison to environments mostly expected for costal structures, real seawater—taken from 2 miles off shore from the Florida State University Marine Laboratory—was also obtained and adjusted for acidity/basicity. To generate the environments, basic chemical aspects had to be considered as explained throughout this deliverable.

Table 1.1 lists all test procedures and references the applicable ASTM standards that were followed throughout the experimental program to characterize the physio-mechanical properties of BFRP rebars. In addition, the table shows how many specimens (per sample group) were needed to reliably measure the material performance.

Because this research targeted the most commonly available and often used FRP rebar sizes, the manufacturer supplied # 3 and # 5 rebars, such that each Rebar Type had two sub-variants (e.g.; Type A # 3, Type B # 3, and Type C # 3). Representative specimen types, characterized throughout this research, are shown in the following Figures 1.2 and 1.3. It can be seen that (at minimum) all rebar types featured a sand coat at the outer surface to improve the bond-to-concrete properties. In addition to surface sand, one product (Type A) also had helical fibers made from polyethylene terephthalate, produced by Dacron. The makeup and the surface enhancement properties of the tested rebars are described in Table 1.2. Because the precise material compositions are proprietary manufacturer information, no more data can be supplied here. However, the BFRP rebar manufacturers were able to provide the raw materials (resin, unsized fiber, and sized fiber) that are used throughout the production process. While unsized fibers (naked basalt fibers) are not used in production and would cause significant issues for the final rebar products, they were included

Table 1.1: Physical and mechanical tests on BFRP rebars

	Test type	Test method	Specimen count	
			Per sample	Total
Physical	Cross-sectional area	ASTM D792	5	40
	Fiber content	ASTM D2584	5	40
	Moisture absorption	ASTM D570	5	40
Mechanical	Tensile strength	ASTM D7205	5	40
	Transverse shear strength	ASTM D7617	5	40
	Apparent horizontal shear strength	ASTM D4475	5	40
	Bond-to-concrete	ACI440.3R,B.3	5	30

(a) Type A (b) Type B (c) Type C

Figure 1.2: Sample pictures of tested BFRP #3 Rebars

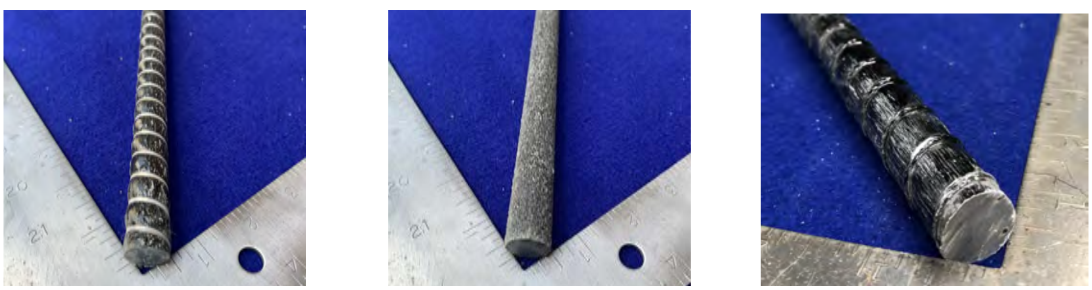

(a) Type A (b) Type B (c) Type C

Figure 1.3: Sample pictures of tested BFRP #5 Rebars

Table 1.2: Physical characteristics of tested BFRP rebars

Name	Cross Section	Surface Enhancement	Resin Type
A	Round (solid)	Sand coat and helical wrap	Epoxy
B	Round (solid)	Sand coat	Epoxy
C	Round (solid)	Helical wrap	Epoxy

in this research project to study the importance and impact of sizing. Nevertheless, it is important to emphasize that a potentially poor performing naked fiber is not (absolutely not) indicative of the final rebar performance, because the sizing significantly alters the behavior of the fiber and the interaction with the resin.

1.2 Generation of Exposure Environments

This section details the experimental procedure followed to develop the chemical environments in which the raw materials and rebars were exposed. As seen in Figure 1.1, a total of 16 different exposure environments were synthetically created for the purpose of this research. To generate the different environments with specific saline levels and certain pH values, the salinity was adjusted first—for the entire amount of solution that required a certain salinity level—before the solutions were subdivided into smaller amounts for the pH adjustment. Then, the solutions were further subdivided to expose all rebars types in a specific category (e.g.: all rebars exposed to 200 Cl^- and 10pH) into individual containers, such that no cross contamination between different rebar types occured. Accordingly, the environments with 4 pH, 7 pH, 10 pH, and 13 pH, with chloride ions varying from 0 Cl^-—20,000 Cl^- were created first. The de-ionized (DeI) water required to generate solutions with 0 Cl^-, 200 Cl^-, and 20,000 Cl^- were collected in large tanks that held the entire amount of the solution that was needed for all specific Cl^-levels. To ensure a stable pH level throughout all solutions of a specific salinity, the de-ionized water was mixed and monitored until no change in pH value occured. After achieving the constant pH, required quantities of the solutions were collected in a smaller tank to create the individual environments (listed in the test matrix above). The required amount of NaCl and NaOH or H_2SO_4 were calculated based on the target pH level and the required volume of deionized water. These substances were weighed accordingly and added to solutions. For example, to create an environment with 10 pH and 200 ppm of Cl^-, first the required amount of NaCl was measured and mixed with the know volume of deionized water. The pH of the deionized water was measured using the pH meter after the NaCl was added because an addition of NaCl may alter the initial pH level. According to the pH value, required amount of NaOH was calculated and weighed to achieve pH 10. Then 90 % of the required NaOH was added to the solution and the pH was measured, before the remaining amount of NaOH was added gradually while the pH was monitored until the required pH was achieved. The above mentioned procedure was followed to create 12 different environments with varying pH and chloride ion content. For the environments with real seawater, water was collected from the Florida State University Marine Laboratory located in St. Teresa, Florida. The seawater was collected at the shore in big tanks at the marine lab and filtered for any impurities like sand. Then collected seawater was separated in required volume for each pH level (4, 7, 10, and 13). Next, the pH of the seawater was adjusted by adding NaOH or H_2SO_4, depending on the desired solution. Each final exposure solution was distributed over 15-2 L large mouth fluorinated bottles to store a separate but chemically identical amount of 1.5 L exposure liquid and a different designated rebar sample—one bottle per rebar type, pH, and salinity. A total of 240 2 L bottles with 16 types of exposures (15 bottles per exposure type — 6 bottles for rebars, 3 bottles for resin, 3 bottles for sized fibers, and 3 bottles for naked fibers) were prepared. Rebars from same production lots were stored in same bottle regardless of size, therefore the six bottles for rebars corresponded to three manufacturers and two lots per manufacturer. This was done, to prevent cross contamination between different rebar components and because various chemical properties of the solutions were monitored to identify and estimate the degradation. Each small bottle (96 in total) designated for rebar samples contain 40 rebar specimens (20-# 3 and 20-# 5) cut in 1 in. in length and 12 rebar specimens (6-# 3 and 6-# 5) cut in 5.5 in. from same manufacturer and identical lot. After placing the samples in the exposure solutions, 2 L bottles (including the solution and material samples) were conditioned to 60 °C (140 °F) to accelerate the potential degradation process. After the two conditioning periods (300 d and 600 d), 10- 1 in. and 3- 5.5 in. rebars will be taken out of exposure solutions and studied for the degradation properties. Two different lengths for the exposed rebar specimens were chosen to study the degradation properties because, small specimens are estimated to degrade more and if the smaller specimens disintegrate before reaching the conditioning period, 5.5 in. rebars will be cut to 1 in. length to study their properties. Figure 1.4 exemplifies the test matrix for one rebar type and one exposure duration (with 16 bottles) on the left and shows the entire test array of created environments in the conditioning chamber on the right.

(a) All 16 environments for Type A Rebars (b) All individual samples in conditioning chamber

Figure 1.4: Individual containers for various exposure solutions

1.3 Tests on Exposure Conditions

To maintain the designed exposure conditions of the storage solutions and to help interpret results from the mechanical and material tests, the conditioning environments will be monitored and analyzed at defined time interval. Different chemical characterization tests will be conducted to quantify and report the chemical properties. All chemical analysis tests — to be conducted on the exposure solutions — are listed in Table 1.3, along with the standard procedures that will be followed for each test. The following subsections detail the experimental procedures for each test.

1.3.1 pH measurements

pH is a measure of the acidic or basic (alkaline) nature of a solution (concentration of the hydrogen ion $[H^+]$ activity in a solution determines the pH). The pH scale ranges from 0 to 14, where 0 signifies acidic nature, a pH of 7 is neutral, and a pH of 14 is the most alkaline. By monitoring the pH level of the exposure solution, the impact of the basalt fiber on the pH environment can be analyzed, whether it turns the solution more acidic or more basic and what to expect when this material is exposed to more aggressive pH conditions.

Figure 1.5 shows the HQ440d Multimeter and a pH probe which were used to measure the pH of the exposure solutions. After connecting the pH probe to the multi meter, the probe was properly cleaned with deionized water and dried using a wiper. Next, the probe was calibrated using pH standard buffer solutions (pH = 4.01, 7.00 and 10.01) to guarantee correct result. About 20 mL of solution was collected in a small glass container. The pH probe was inserted into the sample in such a way that it did not touch the bottom

Table 1.3: Tests on exposure solutions

Test type	Test content	Test standard
Electrometric method	pH	SM4500-H+
Electrical conductivity	Salinity	SM2520-B
Titration method	Alkalinity	SM2320-B
Ion chromatography	Anions	SM4100
Atomic emission spectrometry	Metals	Agilent 4100 MP-AES
Gas chromatographic/mass spectometric method	Biphenol A	SM6040
DO meter	Dissolved oxygen	ASTM D888 - 18
TOC analyzer	Total Organic Carbon	ASTM D7573 - 18ae1

(a) Multimeter

(b) pH probe

Figure 1.5: Multimeter and pH probe

or the surface of that container. After inserting the probe properly, pH measurement was recorded. This procedure was repeated three times per sample and an average value and standard deviation were recorded.

1.3.2 Salinity

Salinity signifies the amount of salt dissolved in a body of water. Salinity is an important factor in determining many aspects of the chemistry of natural water, and is a thermodynamic state variable that, along with temperature and pressure, governs physical characteristics like the density and heat capacity of the water. These parameters may have an affect on the physical characteristics of the basal fiber, which is why salinity was monitored for this research.

A conductivity meter was used to measure the salinity of the exposure solutions. The sample for salinity and dissolved oxygen measurement was the same as for pH measurement. The desired modes, in this case "EC mode" and "Salt" mode were selected on the meter before the measurement was taken to compare the salinity results. The EC probe was cleaned with deionized water and inserted in such a way that it did not touch the bottom or the surface of the container. After inserting the probe properly, the salinity measurements were recorded. This procedure was repeated three times per sample and an average value and standard deviation were recorded.

1.3.3 Alkalinity

Alkalinity is defined as the ability of water to neutralize acid or to absorb hydrogen ions. Alkalinity mainly measures the total concentrations of carbonate ($CO_3{}^{2-}$) and bicarbonate (HCO_3) in the water and has the unit of mg $\frac{CaCO_3}{L}$ Equation 1.1. Since it can be directly used to study the carbon exchange between the rebar samples and exposure solutions. some metals precipitate with carbonate, alkalinity may also help to interpret the metal data.

Alkalinity of the exposure solutions was measured using a HQ440d Multimeter and a pH probe. First, 0.1 N H_2SO_4 stock solution was prepared and a sample of approximately 25 mL was collected in a small beaker. Next, the pH probe was inserted into the sample and the pH reading was recorded while 0.1 N H_2SO_4 stock solution was added to the sample using a micro-liter pipette drop by drop. Acid was added until the pH meter showed 4.5, because when it reached 4.5, the acid consumed all alkalinity inside the sample. Finally the alkalinity was measured using the following equation:

$$\text{Alkalinity, mg } \frac{\text{CaCO}_3}{L} = [2\ \text{CO}_3{}^{2-}]+[\text{HCO}_3{}^{-}]+[\text{OH}^{-}]\text{-}[\text{H}^{+}] = \frac{(A \times N \times 50000)}{(\text{mL sample taken})} \tag{1.1}$$

Where,
A = mL standard acid used
N = normality of standard acid = 0.1N
This procedure was repeated three times for each sample and an average value and standard deviation were recorded.

1.3.4 Anions (Cl^-, $SO_4{}^{2-}$)

Anions are negatively charged ions and are formed from atoms or molecules that have more electrons than protons. Anions often combine with cations to make salts. In this study only 2 types of anions were considered: Cl^- and $SO_4{}^{2-}$. Cl^- is the major anion in the seawater and it accelerates the degradation of BFRP in seawater by participating in the degradation reactions and sulfate is the second major ion in the seawater.

Ion chromatography (IC) was used to measure anions. First an eluent was prepared with certain amount of sodium carbonate, sodium bicarbonate and 2 L of deionized water. The eluent was degassed for approximately 30 min to remove air. The eluent passed through the IC and cleaned the instrument throughout the experiment to maintain proper results. After priming the IC instrument, standards and test samples were prepared. For the standards, stock solutions of both Cl^- and $SO_4{}^{2-}$ were prepared before they were stored in the refrigerator. The prepared stock solutions were diluted in deionized water to make standards of a range of concentrations. Then these standards were inserted into the autosampler for creating the calibration curve. Each sample was diluted and transfered into the IC vials which were then closed using the vial caps. After preparing samples, they were inserted into the autosampler. The final result was obtained by multiplying those recorded concentrations with the dilution factor. This procedure was repeated three times per sample and an average value and standard deviation were recorded.

1.3.5 Metals (Na, K, Ca, Mg, Al, Fe, Cr, Si)

In this project eight metal cations (Na, K, Ca, Mg, Al, Fe, Cr, and Si) are considered for testing because they are the major metal components in basalt and it is expected that the concentration of metals in the exposure solution may increase due to the degradation of basalt.

Agilent 4100 Microwave Plasma-Atomic Emission Spectrometer (MP-AES) was used to measure cation concentration. First, the instrument was prepared for analysis by following the standard procedures. The instrument was calibrated using calibration standards, before the samples were inserted into the side racks. The standards were prepared in different concentrations for all metals that were measured, in this case a total of eight metals. After the standards and samples were inserted, the analysis was initiated. The final results were obtained by multiplying those concentrations with the dilution factor. This procedure was repeated three times per sample and an average value and standard deviation were recorded.

1.3.6 Bisphenol-A

Bisphenol-A is a chemical compound used in the manufacturing of certain food contact materials such as plastics (polycarbonates) and for the production of coatings (epoxy resins). Because in this study resins will be exposed to the exposure solution, bisphenol-A test will inform whether resin is broken down to bisphenol-A and transferred into the exposure solution.

For this test a Gas Chromatograph-Mass Spectrometer (GC-MS) was used. First, an appropriate adsorption-fiber was selected that could extract Bisphenol-A from the sample. Next, for preparing a calibration curve, standards containing certain concentration of Bishenol-A, an internal standard (Bisphenol-A d16), and deionized water were prepared. After preparing the standards and samples in small glass bottles, small magnetic bars were put inside it and the opening was sealed using plastic caps. Next, the bottles containing standards and samples were kept on a hot plate stirrer that had 400 rpm stirring speed at a 60 °C temperature, before the adsorption-fiber was inserted into the sample through the cap. Approximately 19 min were necessary to extract bisphenol-A from the sample. Afterward, the adsorption fiber was inserted into the GC-MS. For appropriate results, this procedure was repeated three times per sample and an average value and standard deviation were recorded.

1.3.7 Dissolved Oxygen

The dissolved oxygen (DO) test returns the amount of oxygen dissolved in the water. It is anticipated that DO may change during the experiment. DO, pH and salinity were measured simultaneously in the same sample, but using different probes. The results will be used to estimate if DO participated in the BFRP degradation reactions.

1.3.8 Total Organic Carbon

Total organic carbon (TOC) is a measure of the total amount of carbon in organic compounds in an aqueous system. It is anticipated that resin and sizing may convert into dissolved organic carbon in high and low pH solutions and therefore they were measured using TOC.

The instrument was set to operate following the standard procedure and the prepared standards were inserted into the autosampler to generate the calibration curve. 40 mL sample was needed for each standard and sample. For accuracy, this procedure was repeated three times per sample and an average value and standard deviation were recorded.

1.4 Tests on Rebars

While the chemical tests to monitor the sensitivity of BFRP rebars to various environments is described above, this section details how each specific mechanical test procedure was conducted and which standard test method was followed to evaluate the individual rebar property. As stated by the test matrix and similar to the chemical test procedures, these tests were conducted on virgin materials and materials that were aged in the different aggressive environments for different time periods.

1.4.1 Cross-Sectional Area

The test procedure to determine the density and specific gravity (relative density) of plastics by displacement methods is described to explain how the rebar diameter (or cross section) was specified for each product. The cross-sectional properties were measured according to ASTM D 792 (ASTM-International, 2015b), while the density of each specimen was calculated via the buoyancy principle. A clean specimen was conditioned for 40 h prior to testing in a temperature range from 21 °C to 25 °C (70 °F to 74 °F) at a relative humidity between 40 % and 60 %. The specimen was then cut to the desired length of 25 mm (1 in.) using an electric precision saw. The length of each curtailed specimen was measured 3 times, at 120° intervals perpendicular to the longitudinal axis of the FRP rebar, and the average value was noted for density calculations. Afterwards, the weight of dry and conditioned specimen was measured using an electronic balance and recorded to the nearest 0.05 g (0.0017 oz.). The recorded weight of the curtailed specimen was measured to be no less than 10 g (0.352 oz.) and the value was used as the initial specimen weight, (W_i), needed for density calculations. A glass beaker of known volume was used as an immersion vessel to hold the water in which the sample was submerged . However, the immersion vessel was tared to obtain the weight of the sample under buoyancy only. The temperature of the water bath was monitored for each test and constant water temperatures of 21 °C to 25 °C (70 °F to 74 °F) were maintained throughout all experiments. A corrosion-resistant copper wire was used as a sample holder and attached to the fixture that was independent of the water bath/vessel but introduced the forces to the scale, the specimen was carefully attached to one end of the copper wire. Then, the weight of the specimen along with the copper wire was measured and recorded (Specimen + wire, W_{s+w}). The immersion vessel was placed on the support (independent of the weighing mechanism), and the specimen was completely submerged in the water with the help of the copper wire. To remove any entrapped air or air bubbles at the surface of the FRP rebar, the specimen was carefully rubbed with the wire across the surface and submerged in a rotating motion. Any water that was displaced onto the scale was wiped without disturbing the immersion vessel. The weight of the submerged specimen was measured and recorded as final weight (W_f). Density measurements were determined via the buoyancy principle and the cross-sectional dimensions were calculated by dividing the determined volume by the measured specimen length. For reliability of test results and to obtain representative values for the BFRP rebar product as a whole, the test was repeated five times for specimens taken from different sections of the production lot and the average value was assigned.

1.4.2 Fiber Content Test — Ignition Loss

The procedure for ignition loss test for cured reinforced resins is explained here to describe how the fiber content for the tested basalt FRP rebars was determined. ASTM D 2584 -11(ASTM-International, 2011) outlines this procedure and details the required conditions. Similar to the specimen preparation for the cross-sectional dimension experiments, the specimens for this procedure were also conditioned in a temperature range from 21 °C to 25 °C (70 °F to 74 °F) at a relative humidity between 40 % and 60 %, for at least 40 hours prior to testing. The conditioned sample was then cut to the desired length of 25 mm (1 in.) with a precision of 0.05 mm (0.0019 in.). The weight of the conditioned sample (W_s), was then recorded to the nearest 0.05 g (0.0017 oz.) using an electronic balance. This weight was used as the 100 % reference value for calculating the fiber and resin contents (relative to the initial weight). Likewise, a clean and oven-dried crucible was weighed (W_c) to the nearest 0.05 g (0.0017 oz.) to obtain the initial weight of the sample holder. The FRP rebar specimen was transferred to the crucible and the total weight of the specimen and the crucible (W_i) was recorded to the nearest 0.05 g (0.0017 oz.). To burn off all resin, the crucible (of known mass) along with the specimen were exposed to a temperature of 542 °C to 593 °C (1000 °F to 1100 °F) in a muffle furnace until the specimens reached a constant weight. The crucible was then carefully removed from the muffle furnace and allowed to cool down to room temperature, before the cooled crucible including the remaining material was weighed using a precision electronic balance. This weight was recorded as final weight (W_f). Because the rebar products were made with sand at the surface for bond enhancement, the weight of the sand (W_s) was recorded and subtracted from the initial weight of the crucible and the specimen to obtain comparable and absolute fiber content percentages. Because fibers (and sand) are not susceptible to loss on ignition, the reduction in weight due to the burning process is equivalent to the weight of resin, and hence, the percentage of fibers was determined through the difference in weight before and after the burning process. For reliability of test results and to obtain representative values for the BFRP rebar product as a whole, the test was repeated five times for specimens taken from different sections of the production lot and the average value was assigned.

1.4.3 Moisture Absorption Test

The test procedure described in ASTM D 5229 (ASTM, 2014) defines the standard method for determining the moisture absorption characteristics of FRP and is an indicator of porosity. This paragraph explains how the porosity of the tested rebars was determined and calculated. ASTM D 5229 offers seven different test procedures (A through E, Y, and Z) to assign moisture absorption properties for FRP in different environments. Procedure A is most commonly used, and was used for this research project. Each specimen was first oven dried for 48 h to eliminate moisture entrapped in the pores or at the surface. The dried and conditioned specimens were placed in storage bags to ensure that no moisture contaminated the specimens. Three diameter measurements were taken at 120° intervals, perpendicular to the longitudinal axis of the FRP rebar, and those measurements were recorded to the nearest 0.001 mm ($\frac{4}{10\,000}$ in.). Then, each specimen was weighed with a precision of 0.05 g (0.0017 oz.) in its dry state and recorded as W_i. The specimens were then submerged in distilled water. The water along with the submerged specimens were stored in an air-circulated oven to maintain a temperature of 50 °C (122 °F) throughout the entire duration of the conditioning. First weight measurements to record W_1 after water conditioning were taken after two weeks. To obtain additional measurements, the specimens were removed from the water bath in two-week intervals (continuous conditioning) and surface dried with a fresh paper towel until no free water remained on the surface of the FRP rebar. All intermediate measurements and the final weight of each specimen (W_f) were measured and recorded to the nearest 0.05 g (0.0017 oz.). This procedure was repeated and weight gains were monitored until three consecutive two-week measurements did not differ by more than 0.02 % from one another. For reliability of test results and to obtain representative values for the BFRP rebar product as a whole, the test was repeated five times for specimens taken from different sections of the production lot and the average value was assigned.

1.4.4 Transverse Shear Strength Test

ASTM D 7617 (ASTM-International, 2012b) was used in the process of testing and analyzing the transverse shear strength data. Before testing, the specimens were conditioned according to the ASTM D 5229 (ASTM, 2014). The conditioned specimen were then cut to a minimum length of 225 mm (8.85 in.) so that they fit in the shearing apparatus, which is a device that produces double shear on the FRP rebar specimen. The conditioned and curtailed bars were placed inside the shear test device and loaded with a displacement rate such that the test continued for at least 1 minute, but not more than 10 minutes until the force reached 70 % of the ultimate load. The transverse shear strength was determined using the ultimate load and the nominal nominal cross-sectional area of the specimen.

1.4.5 Apparent Horizontal Shear Test

The FRP rebar products were tested for the apparent horizontal shear properties and this test was conducted according to ASTM D 4475 (ASTM-International, 2012a) standards. First, the diameter at the center of the specimen was recorded and the specimens were conditioned at a temperature range from 21 °C to 25 °C (69.8 °F to 77 °F) and a moisture content between 40 % and 60 % before they were cut to a length of approximately five times the diameter. The horizontal shear strength was assessed through a three-point load test over a span length that was short enough to avoid bending failure. The load was applied at the center of specimen with a displacement rate of 1.3 $\frac{\text{mm}}{\text{min}}$ (0.05 $\frac{\text{in.}}{\text{min}}$) until the shear failure was reached via horizontal delamination (failure of the resin or resin-fiber interface). The ultimate load and the break type (number of fracture surfaces) were recorded and analyzed. For reliability of test results and to meet the requirements listed in FDOT Specifications, Section 932, a minimum of five specimen per sample were tested.

1.4.6 Tensile Strength and Modulus Test

The rebars were tested according to the ASTM D 7205, which describes a specific test method for specimen preparation and testing of FRP rebars. It details how to anchor and grip the rebar specimen via steel pipe anchors at both ends, which is necessary because of the low shear and crushing strength of FRP rebars as such anchors prevent the rebar from failing in shear before reaching the ultimate tensile strength. Otherwise, the grip mechanism of standard test machines would lead to a premature (transverse) failure of the specimen. The anchors for this research project were potted with expansive grout to transfer the force from the testing machine into the rebar through compression and friction between the rebar surface and the grout. The dimensions of the anchors relate to the rebar diameter and the free specimen length between the anchors was set to 40 times the rebar diameter. After the grout in the anchors was cured for a minimum of seven days, the specimens were fixed in the MTS test frame. After the specimen was placed into the fixture and aligned properly by the locking plates, the crossbar of the machine was locked for safety purposes. An initial load of 1 kN (0.225 kip) was applied to the bar to guarantee identical stiffness at the onset of each test. The next step was to place the extensometer with two little rubber bands in the middle of the free specimen length of the rebar. After the extensometer was in place, the safety pin was pulled out and the extensometer was connected to the computer to measure the displacement. The specimen was installed and the test was initiated. The load rates were chosen to target a failure time between 60 s (1 min) and 600 s (10 min) as defined by ASTM D 7205 / D 7205 (ASTM-International, 2015a). After starting the test program, the force versus displacement and the strain data were monitored continuously at a 10 Hz frequency. According to ASTM D 7205, the tensile chord modulus of elasticity should be calculated from the strain range of the lower half of the stress-strain curve, between 0.1 % and 0.3 % of strain. To protect the extensometer, it was removed at around 10 % displacement (without interrupting the load application) before the sample failed and possibly damaged the extensometer. The testing machine stopped automatically when the force dropped by 85 %. For repeatability, a minimum of five specimen per sample group were tested.

1.4.7 Bond-to-Concrete Strength Test

The bond-to-concrete properties of the rebars were evaluated via pullout testing according to ASTM D7913 (ASTM International, 2014). The bond strength experiments were conducted under standard laboratory conditions within (23 ± 2) °C [(73 ± 5) °F] and (50 ± 10) % relative humidity, using a 300 kN (66 kip) hydraulically controlled load frame. First, the specimens were cleaned and installed in the test frame and an initial seating load of 272 kN (600 lbs.) was applied to generate sufficient stiffness in the system. Then the LSCTs, which were needed to measure the rebar slip at both ends (the so-called free and load ends). Once the setup was safe, a static force was continuously applied via a displacement rate of $0.75\,\frac{\text{mm}}{\text{min}}$ ($0.03\,\frac{\text{in.}}{\text{min}}$) and the raw data was recorded with 1000 Hz until the measured force decreased significantly (more than 50 %) and the slippage at the free end of the bar measured at least 2.5 mm (0.1 in.). After each test was completed, the concrete block was split open to analyze the failure mode and to measure the precise bond length of each specimen. For repeatability, a minimum of five specimen per sample group were tested.

Chapter 2

Aggressive Environments — Solution Properties

According to the test matrix, 16 different solutions—with various pH-values and salinity levels—were generated to expose the raw constituents and composite basalt rebar materials to aggressive environments. While each specific solution (with a defined ph-value and salinity-level) was eventually distributed over various bottles and containers, the entire required amount for each solution was created in a single (well mixed) batch to guarantee identical exposure conditions across the various materials and components within each particular solution type (c.f. test matrix). The actual mixing process is detailed in the previous deliverable, but this chapter specifies how the solutions were tested and evaluated for various chemical properties. This step was necessary for quality control and to generate baseline values, before the rebar materials were submerged in the corresponding solution.

2.1 Introduction

The measurement of pH, salinity, dissolved oxygen and anions were determined according to the 'Standard Methods' for examining water and wastewater properties (Rice et al., 2012). For each parameter, triplicate samples were measured and the corresponding minimum, maximum, and average concentrations were recorded. These measurements were completed immediately before the unsized fiber, sized fiber, resin plates and rebars were exposed to the solutions. Therefore, the results presented in the following section (Section 2.2) are the representation of baseline data (i.e., the 0 day data). By examining the changes of the exposure solution water chemistry, affects of the different exposure solutions on the fibers, resins and rebars after 300 days and 600 days will be studied.

2.2 Results

Results for pH and salinity are summarized in Table 2.1. All pH and salinity results were very close to the target values (theoretical values in the first two columns). The variation between the triplicate measurements were minimal.

The results for dissolved oxygen and anions are summarized in Table 2.2. The concentrations for dissolved oxygen did not vary for the 16 mixes and they were close to the saturated concentration. All measured chloride concentrations were similar to the target concentrations. For the exposure solutions with a pH-value of 4, sulfate concentrations were measured because H_2SO_4 was added to lower the pH to 4.

Table 2.1: pH and Salinity results of exposure solutions

Exposure Target		pH			Salinity		
pH	cl^-				mg/L		
	ppm	$\wedge$	$\vee$	μ	$\wedge$	$\vee$	μ
4	0	3.99	4.00	3.99	9.70	9.80	9.73
4	200	3.99	4.00	4.00	343.00	344.00	343.33
4	20000	3.98	3.99	3.99	32 970.00	32 980.00	32 976.70
4	Seawater	4.01	4.02	4.02	33 690.00	33 710.00	33 696.70
7	0	7.01	7.02	7.02	5.50	5.50	5.50
7	200	7.00	7.01	7.00	335.00	336.00	335.67
7	20000	7.00	7.01	7.01	32 950.00	32 960.00	32 953.30
7	Seawater	7.01	7.03	7.02	33 710.00	33 730.00	33 723.30
10	0	10.00	10.01	10.00	6.90	6.90	6.90
10	200	10.01	10.02	10.01	338.00	339.00	338.70
10	20000	9.99	10.00	10.00	32 960.00	32 970.00	32 966.70
10	Seawater	10.01	10.02	10.02	34 540.00	34 560.00	34 546.70
13	0	12.99	13.00	12.99	4005.00	4010.00	4008.33
13	200	13.01	13.03	13.02	4333.00	4336.00	4334.30
13	20000	13.00	13.01	13.00	36 970.00	36 980.00	36 973.30
13	Seawater	12.98	12.99	12.99	36 600.00	36 610.00	36 596.70

Table 2.2: Dissolved oxygen and Anions results of exposure solutions

Exposure Target		DissolvedOxygen			Anions					
					Chloride			Sulfate		
pH	cl^-	mg/L			mg/L			mg/L		
	ppm	$\wedge$	$\vee$	μ	$\wedge$	$\vee$	μ	$\wedge$	$\vee$	μ
4	0	8.89	8.90	8.89	< 0.08	< 0.08	< 0.08	6.01	6.04	6.02
4	200	8.81	8.82	8.82	201.09	201.12	201.10	6.17	6.21	6.20
4	20000	8.76	8.80	8.77	20 008.10	20 010.24	20 008.81	6.35	6.36	6.36
4	Seawater	8.57	8.60	8.58	19 948.70	19 950.34	19 949.25	2653.95	2658.31	2655.40
7	0	8.86	8.87	8.87	< 0.08	< 0.08	< 0.08	< 0.50	< 0.50	< 0.50
7	200	8.80	8.81	8.82	201.11	201.11	201.11	< 0.50	< 0.50	< 0.50
7	20000	8.74	8.78	8.76	20 007.97	20 010.43	20 009.61	< 0.50	< 0.50	< 0.50
7	Seawater	8.55	8.57	8.56	19 947.90	19 951.67	19 949.42	2646.85	2648.89	2647.78
10	0	8.85	8.87	8.86	< 0.08	< 0.08	< 0.08	< 0.50	< 0.50	< 0.50
10	200	8.78	8.81	8.79	201.12	201.14	201.13	< 0.50	< 0.50	< 0.50
10	20000	8.73	8.75	8.74	20 009.35	20 011.49	20 010.06	< 0.50	< 0.50	< 0.50
10	Seawater	8.55	8.56	8.56	19 952.89	19 955.78	19 954.82	2647.59	2651.11	2649.94
13	0	8.83	8.84	8.84	< 0.08	< 0.08	< 0.08	< 0.50	< 0.50	< 0.50
13	200	8.75	8.79	8.77	201.13	201.14	201.14	< 0.50	< 0.50	< 0.50
13	20000	8.70	8.71	8.70	20 008.19	20 011.67	20 009.35	< 0.50	< 0.50	< 0.50
13	Seawater	8.52	8.54	8.53	19 948.96	19 953.71	19 950.54	2647.25	2651.89	2648.79

Chapter 3

Physical Properties

3.1 Introduction

The performance evaluation of virgin basalt fiber reinforced polymer (BFRP) rebars is summarized in this chapter. The following results were obtained at the FAMU-FSU College of Engineering in the Structures and Materials laboratories. All tests were conducted in accordance with the relevant American Society for Testing and Materials (ASTM) test protocol. The collected raw data were analyzed with the engineering software R-statistics[1] and R-Studio[2]. The results in this chapter are presented in graphs to visualize individual specimen data, while tables are used to summarize the statistical data of each test sample (rebar type). For clarity, each property was individually studied; accordingly, each material characteristic is presented separately.

3.2 Cross-Sectional Properties

The effective rebar diameter was measured according to the ASTM D 792-13. Due to the variety of FRP rebars on the market and depending on the proprietary production methods, rebars with different surface enhancement may vary significantly and deviate from the given nominal diameter. Table 3.1 below lists the results of water displacement method according to the ASTM D 792-13 of all the rebar products.

[1] R.app GUI 1.70 (7434 El Capitan build), S. Urbanek & H.-J. Bibiko, R Foundation for Statistical Computing, 2016
[2] Version 1.1.383 2009-2017 RStudio, Inc.

Table 3.1: Statistical evaluation of diameter measurements for rebar size # 3 and # 5

Rebar			$\wedge$	$\vee$	μ	σ	CV
Type	Size	Lot	mm	mm	mm	mm	%
A	# 3	1	10.67	10.93	10.76	0.11	0.99
B	# 3	1	9.84	10.47	10.31	0.26	2.56
C	# 3	1	10.46	10.80	10.55	0.14	1.38
A	# 3	2	10.41	10.94	10.70	0.20	1.89
B	# 3	2	10.57	10.83	10.72	0.11	1.05
C	# 3	2	16.24	16.41	16.30	0.06	0.39
A	# 5	1	16.66	16.79	16.71	0.05	0.30
B	# 5	1	17.52	17.59	17.56	0.03	0.19
C	# 5	1	10.32	10.34	10.35	0.00	0.09
A	# 5	2	16.26	16.52	16.43	0.10	0.60
B	# 5	2	17.53	17.65	17.57	0.05	0.30
C	# 5	2	16.38	16.55	16.48	0.06	0.41

3.3 Fiber Content

The fiber content by weight of the rebars was calculated according to ASTM D 2584 -11 (ASTM-International, 2011). The measured fiber content results are plotted in Figure 3.1. The bar chart was generated to compare

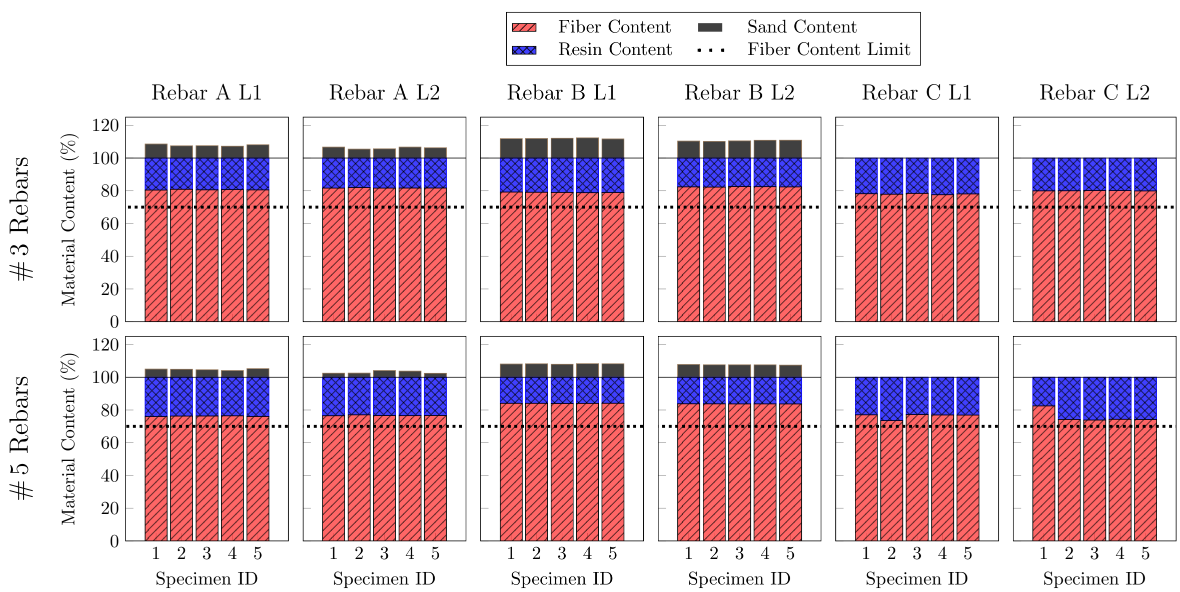

Figure 3.1: Fiber content percentage of rebars from all manufacturers

the different rebar types against each other and to compare the different rebar sizes. Each row in the plot indicates a specific rebar size, while each column represents a different rebar type. The bars represent individual specimens. The red hatched part of the bars indicates the fiber content in percentage, the blue crosshatched part represents the percentage of resin, and the black part represents the amount of sand that was applied to the rebar surface to increase the bond-to-concrete performance. Since the weight of the sand surface enhancement has a relative higher contribution (percentage wise) on smaller specimens, the percentage weight on # 3 rebars is higher than # 5 rebars as presented in bar chart. The 100 % values for these rebars are based on total specimen weight minus the sand content. The dashed line at the 70 % mark shows the AC454 and FDOT currently accepted minimum fiber content for FRP rebars. It can be seen that all individual rebar specimens met the minimum requirement for the fiber content. Overall, the measured fiber content results show that the production quality was consistent for all rebar types and sizes (within each rebar product).

The following Figure 3.2 presents typical closeup pictures for individual test specimens of rebar types A and B. These pictures show # 3 rebar from Type A and # 5 rebar from Type B.

(a) Type A

(b) Type B

Figure 3.2: Fiber content specimen of rebars after test

3.4 Moisture Absorption

The moisture absorption property of rebars was tested in accordance with ASTM D 5229 (ASTM, 2014). The graph plotted in Figure 3.3 represents weight change of all tested rebar types stored in distilled water over a test period of 98 d. It can be seen in the graph that all rebar types showed comparable moisture absorption behavior. All the rebar types satisfied the AC454 limitations for the absorption limit of 0.25 % in first 24 hours of exposure.

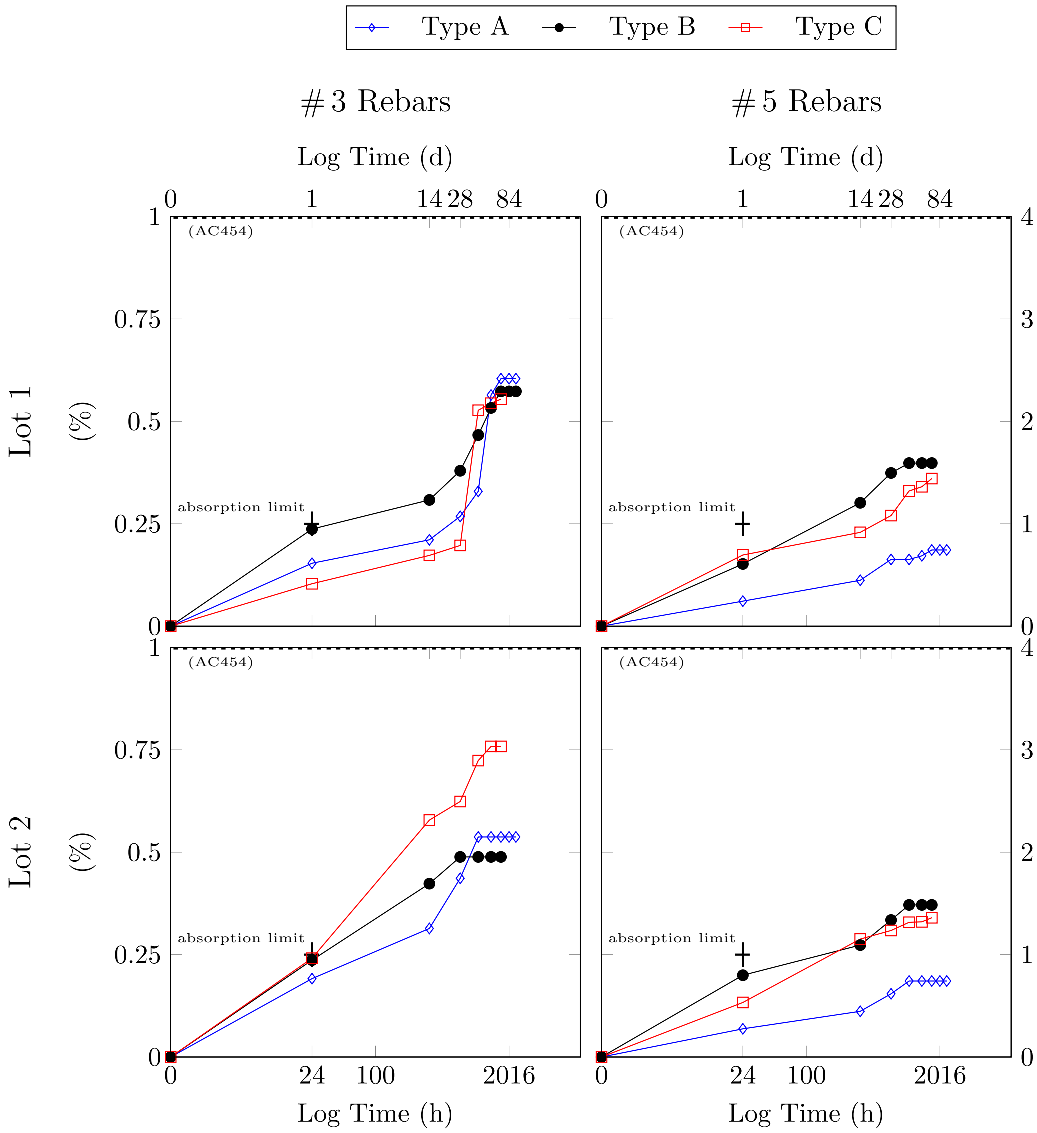

Figure 3.3: Moisture absorption results of rebars from all manufacturers

Chapter 4

Mechanical Properties

4.1 Transverse Shear Test

ASTM D 7617 (ASTM-International, 2012b) was used in the process of testing and analyzing the transverse shear strength of the rebars. Tested and processed data are plotted in the following sections 4.1.1 and 4.1.2.

4.1.1 Load-Displacement

The graphs plotted in Figures 4.1, 4.2, 4.3, 4.4, 4.5, and 4.6 show the load-displacement behavior recorded during the transverse shear tests of # 3 and # 5 rebars for all rebar types tested in this study. The x-axis of the graph represents the cross-head extension or the relative displacement between the edges of the directly sheared specimen, while the y-axis shows the measured force throughout the load application period.

The Graph in figure 4.1 shows a linear behavior until it reaches the ultimate failure load. It can be seen

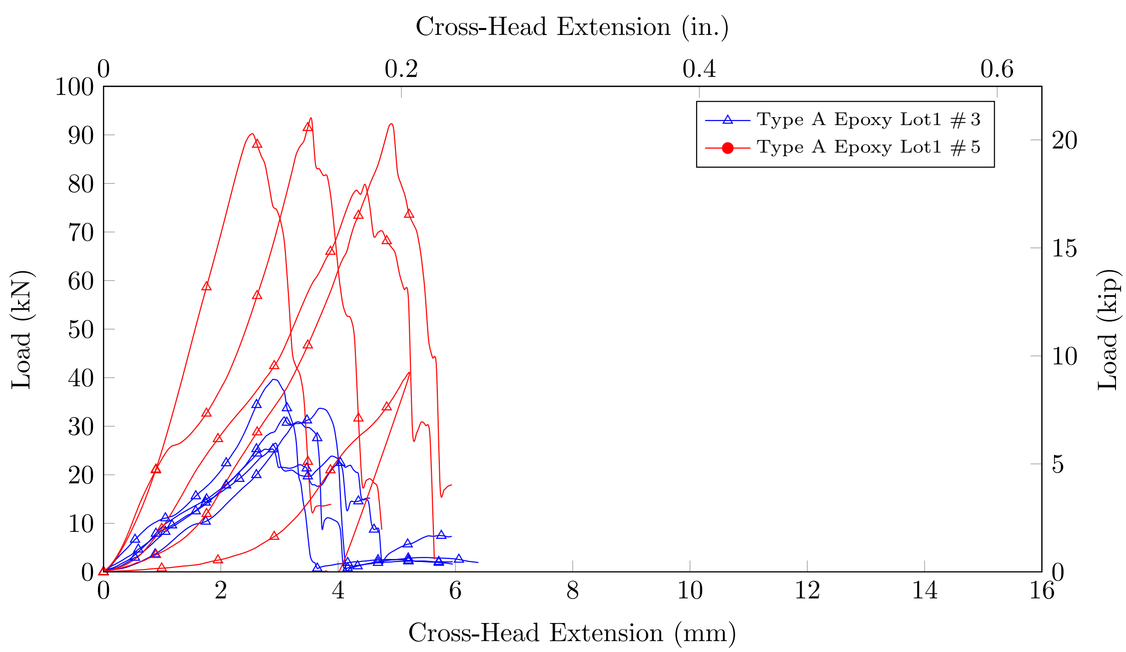

Figure 4.1: Extension-transverse shear load behavior of Type A rebars Lot 1 size 3 and 5

that # 5 sized rebar sustained higher load in comparison with # 3 rebars. All the # 3 rebars sustained a consistent load while # 5 rebars sustained same peak load but the extension of the rebars varied. The graph in Figure 4.2 shows a comparison between the load and the displacement for transverse shear strength of # 3 and # 5 rebars Lot 1 from Type B rebar. It can be seen that the graph had a linear behavior until it

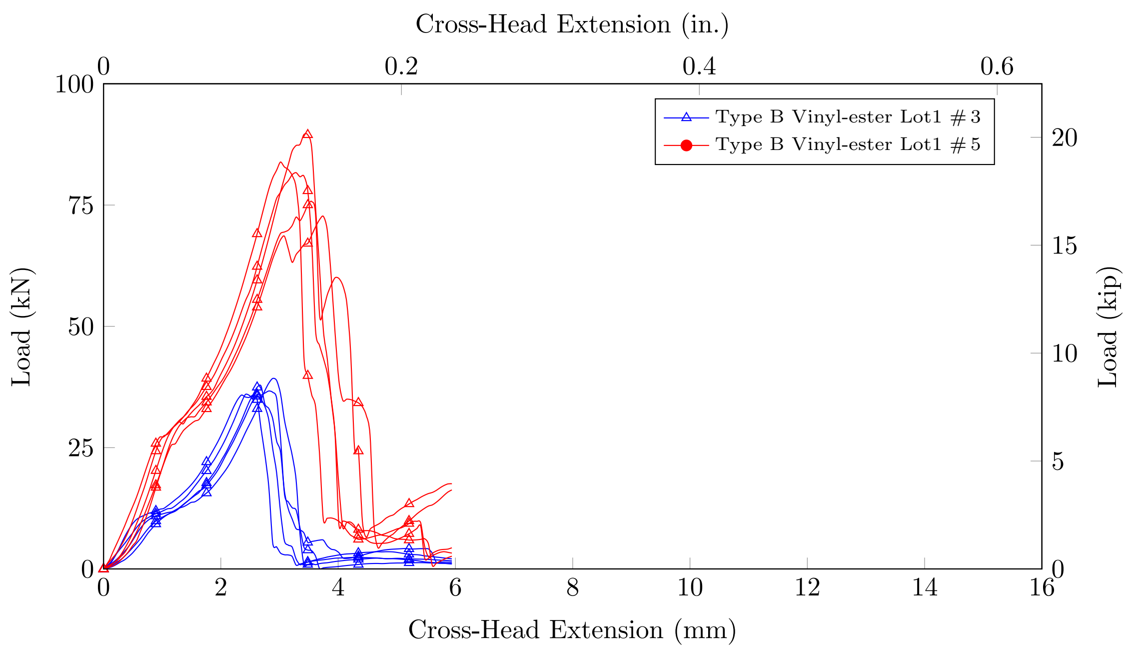

Figure 4.2: Extension-transverse shear load behavior of Type B rebars Lot 1 size 3 and 5

reached the ultimate failure load. All the rebars sizes sustained a consistent load with similar extension. The Graph in Figure 4.3 shows the load - displacement behavior of Type C rebars. Linearity can be seen until it reaches the ultimate failure load. It can be seen that # 5 sized rebar sustained higher load in comparison

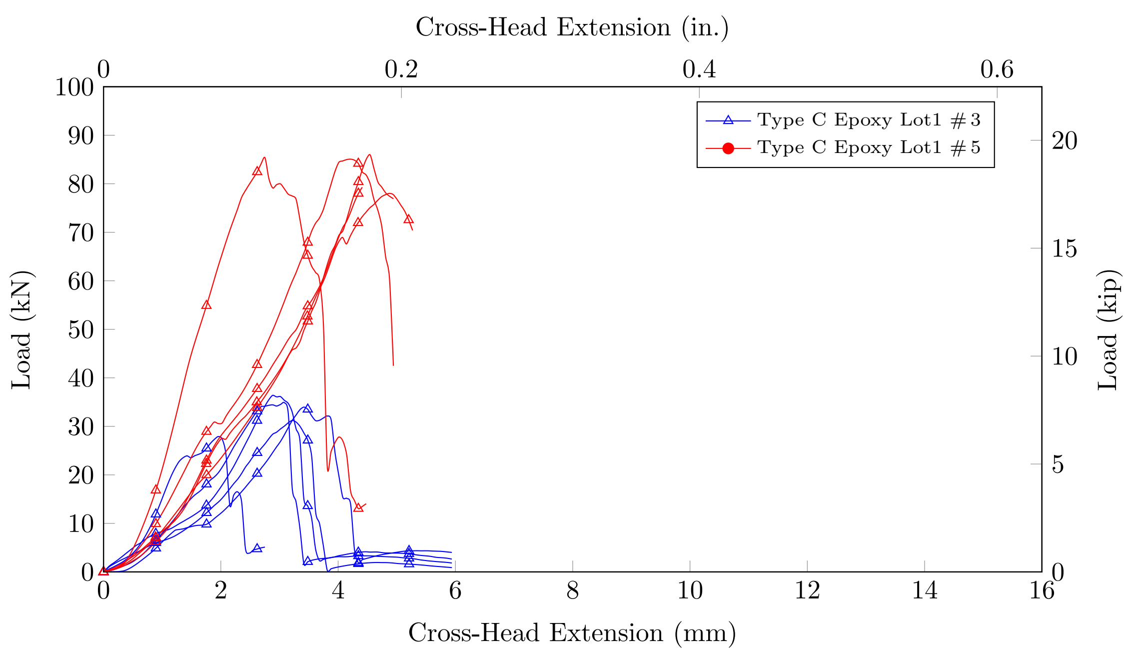

Figure 4.3: Extension-transverse shear load behavior of Type C rebars Lot 1 size 3 and 5

with # 3 rebars. The graph in Figure 4.4 presents a comparison between the load and the displacement for of transverse shear strength of # 3 and # 5 rebars from Type A from Lot 2. The graph shows a linear

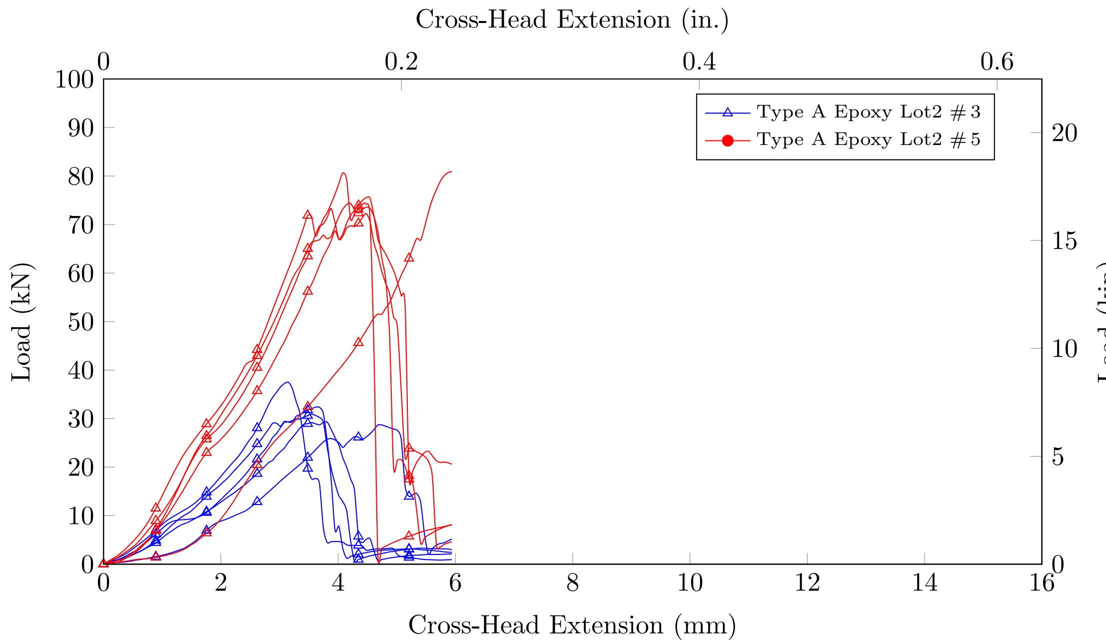

Figure 4.4: Extension-transverse shear load behavior of Type A rebars Lot 2 size 3 and 5

behavior until it reached approximately 90% of the ultimate failure load. The visualized data in Figure 4.5 show the load-displacement behavior for transverse shear strength of # 3 and # 5 rebars Lot 2 from Type B rebar. It can be seen that the material behaved linearly until approximately 90 % of the ultimate failure

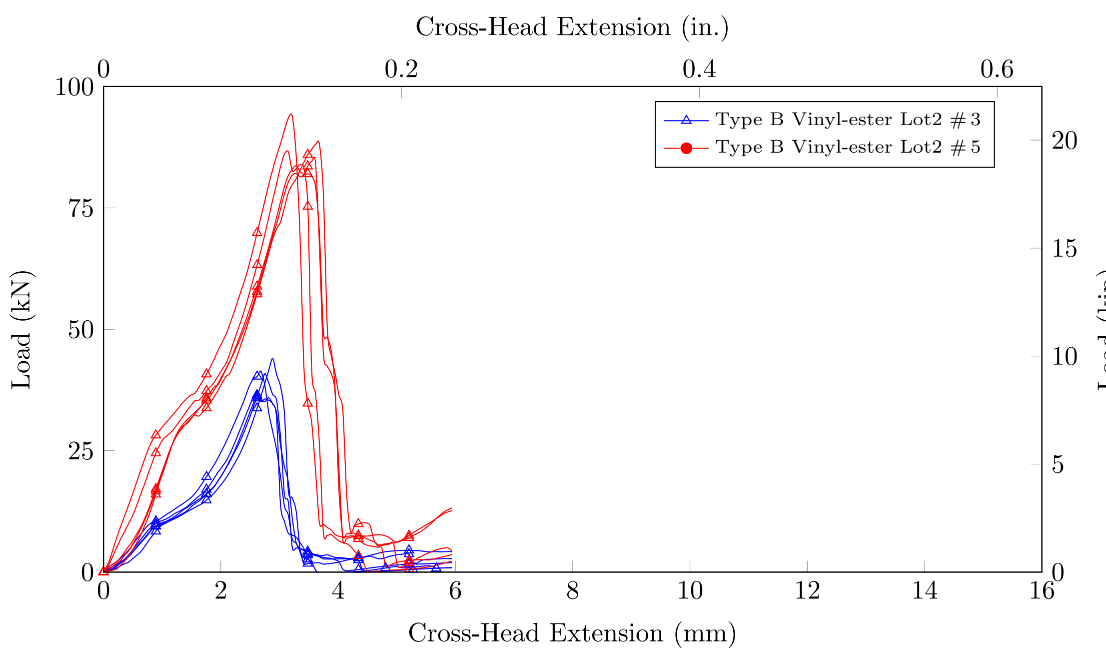

Figure 4.5: Extension-transverse shear load behavior of Type B rebars Lot 2 size 3 and 5

load was reached. All the # 3 rebars sustained a consistent load while # 5 rebars sustained same peak load but the extension of the rebars varied. The graph in Figure 4.6 shows a comparison between the load and the displacement for transverse shear strength of # 3 and # 5 rebars from Lot 2. The graph shows a linear

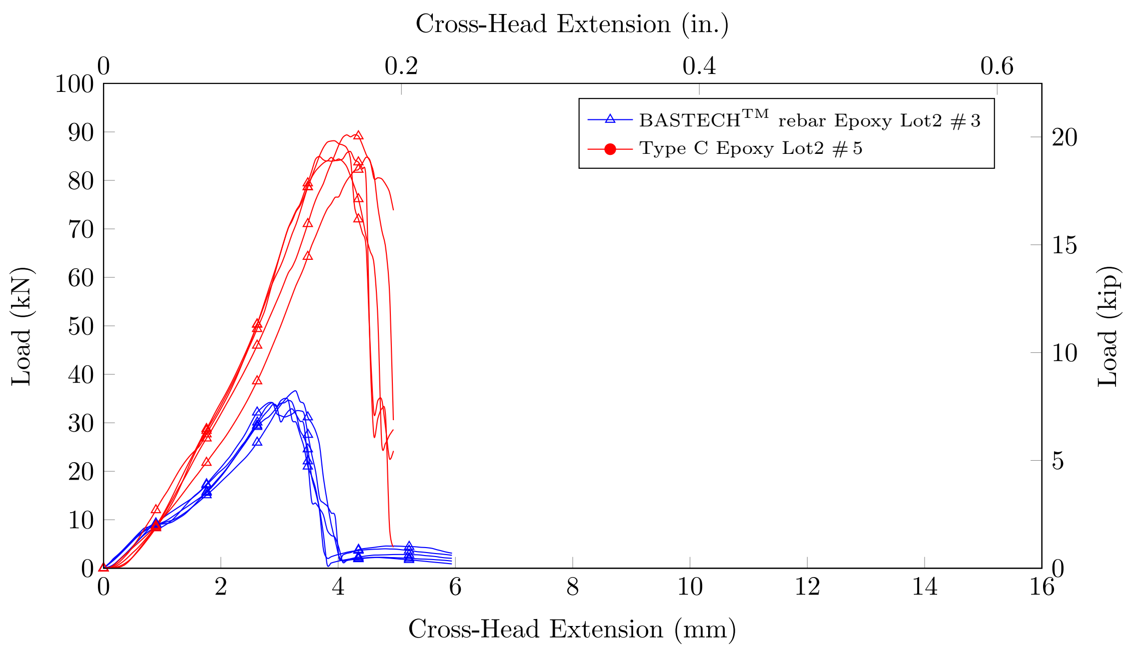

Figure 4.6: Extension-transverse shear load behavior of Type C rebars Lot 2 size 3 and 5

behavior until it reached approximately 90% of the ultimate failure load.

4.1.2 Stress-Displacement

The results obtained from the transverse test was properly reduced and analyzed. These results are shown via graphs and table. The graphs in Figures 4.7, 4.8, 4.9, 4.10, 4.11, and 4.12 compare the stress-displacement behavior of transverse shear test of # 3 and # 5 rebars from all rebar types that were tested for this research project. The data along the x-axis represents the cross-head extension or the direct shear displacement, while the y-axis signifies the measured shear stress.

The data in Figure 4.7 show that the material behaved nearly linearly until the ultimate failure load was reached. It can be seen in Figure 4.7 that the stress-strain behavior of all rebars was close but not identical—specifically, it varied significantly for rebar number # 5.

The graph in Figure 4.8 presents the stress-displacement behavior of transverse shear test of rebar Type B Lot 1. From the stress-strain behavior of rebar Type B as shown in Figure 4.8, it can be seen that the rebars underwent similar failure behavior. The graph in Figure 4.9 compares the stress - strain behavior of Type C rebar from Lot 1. It shows the linearity of tested rebar until the ultimate failure load was reached. It can be seen in Figure 4.9 that the stress-strain behavior of all rebars was close but not identical—specifically, it varied significantly for rebar number # 5. The graph in Figure 4.10 presents the stress-displacement behavior of transverse shear test of rebar Type A Lot 2. The graphs display a mostly linear behavior until the ultimate failure load was reached. Figure 4.11 shows the stress-displacement behavior of transverse shear test of rebar Type B Lot 2. It can be seen that the data represented a nearly linear behavior until the ultimate failure load was attained. The stress-displacement behavior of failed rebar specimen from both types from Lot 2 in Figures 4.10 and 4.11 show that, although the ultimate failure capacity of the rebars varied significantly, all the rebar samples failed in a identical manner. The graph in Figure 4.12 presents the stress-displacement

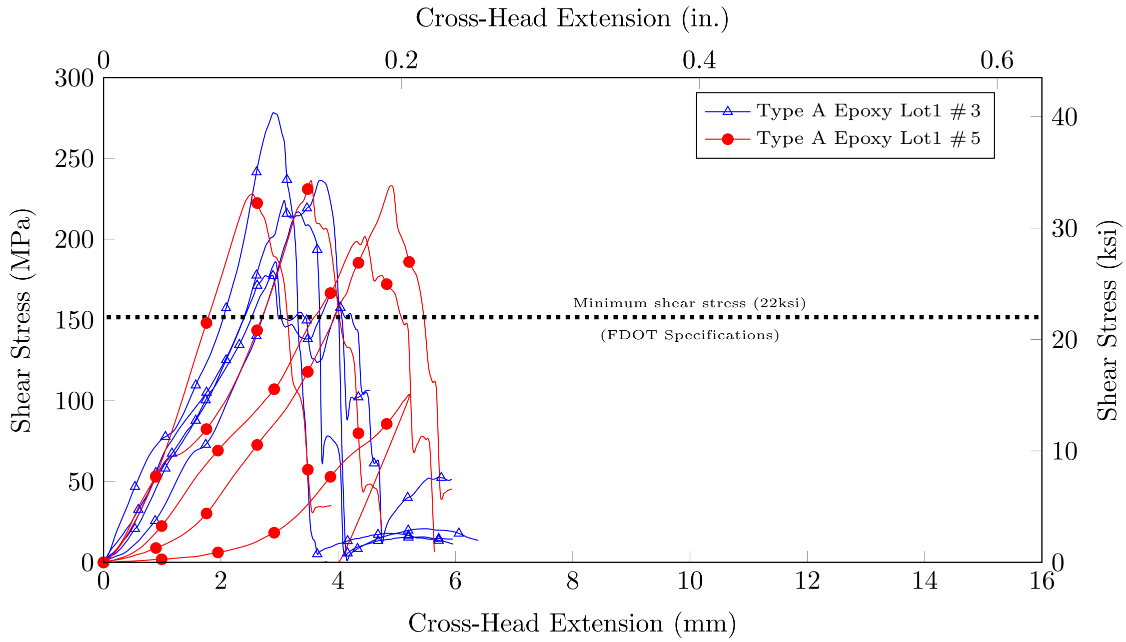

Figure 4.7: Transverse shear stress-extension behavior of rebar Type A Lot 1 size 3 and 5

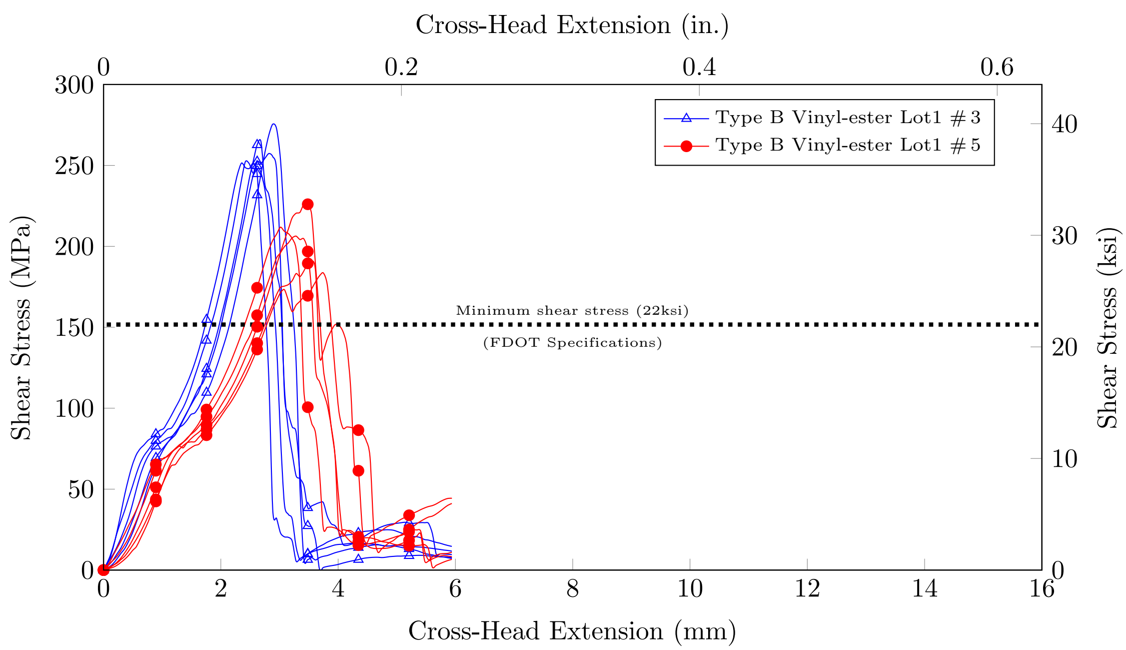

Figure 4.8: Transverse shear stress-extension results of rebar Type B Lot 1 size 3 and 5

behavior of transverse shear test of Lot 2 rebars from Type C manufacturer. From the stress-displacement behavior of rebar as shown in Figure 4.12, it can be seen that the rebars underwent similar failure behavior.

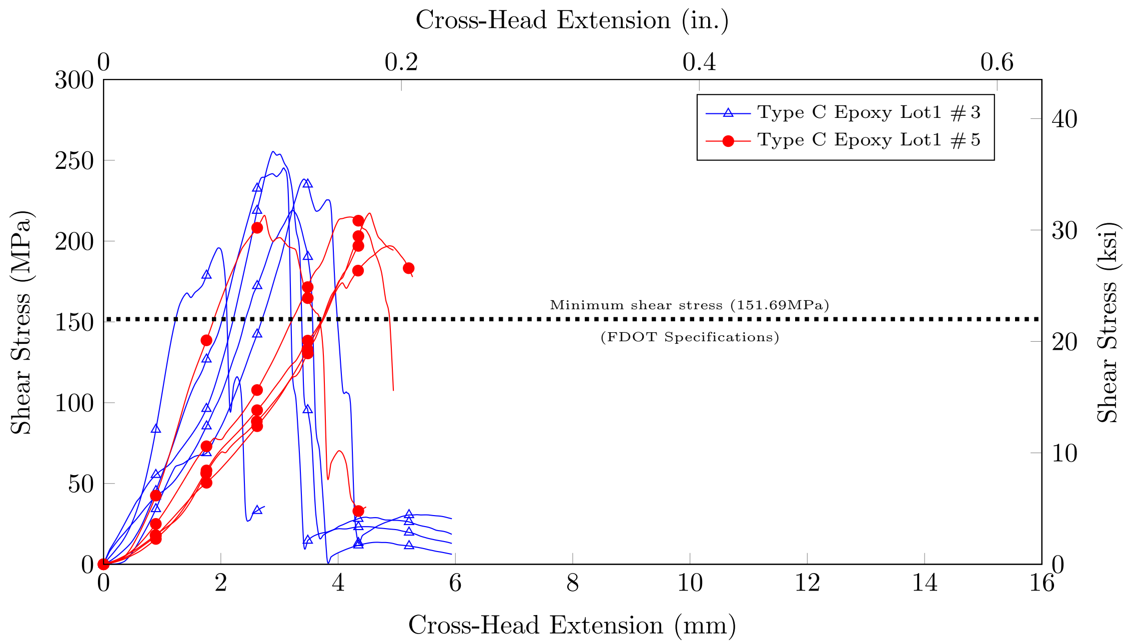

Figure 4.9: Transverse shear stress-extension results of Type C rebar Lot 1 size 3 and 5

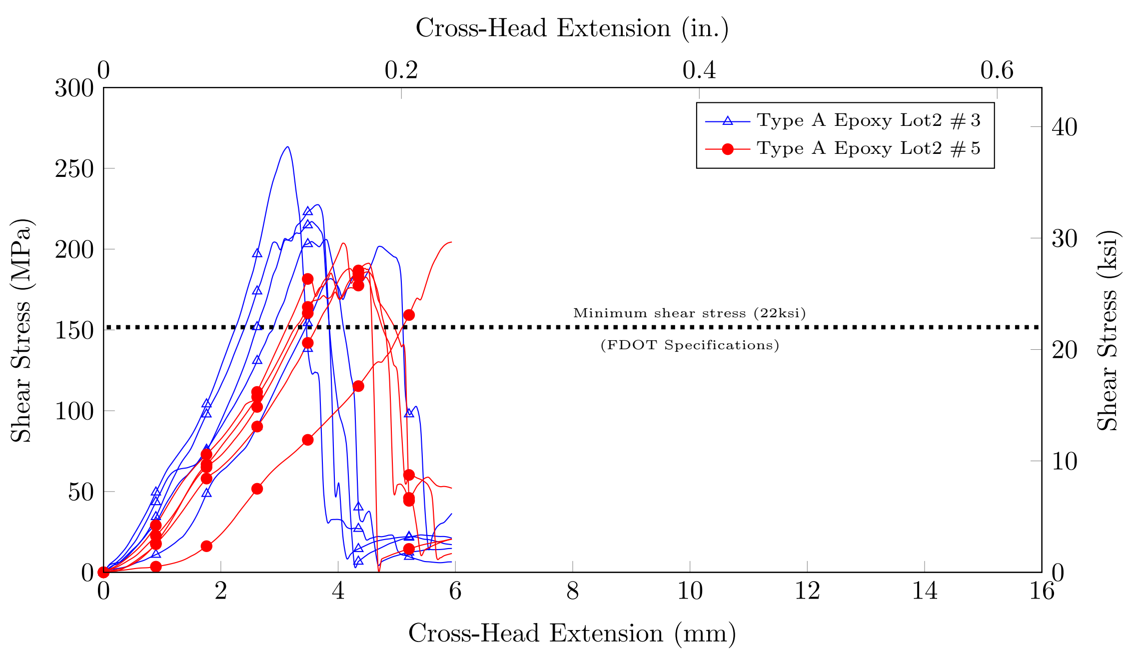

Figure 4.10: Transverse shear stress-extension behavior of rebar Type A Lot 2 size 3 and 5

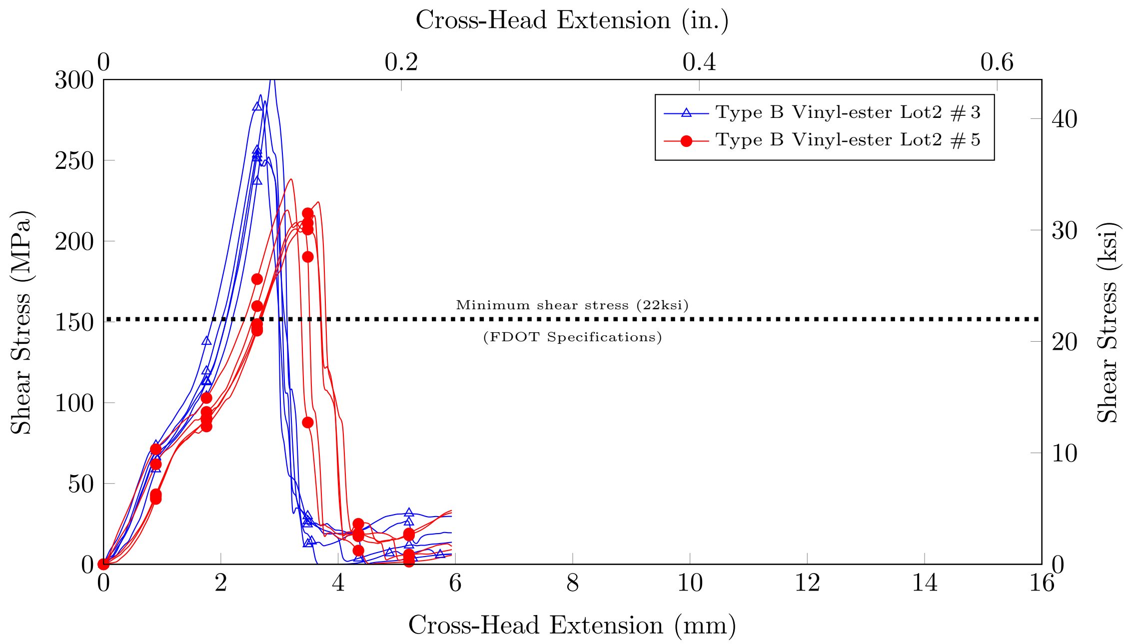

Figure 4.11: Transverse shear stress-extension results of rebar Type B Lot 2 size 3 and 5

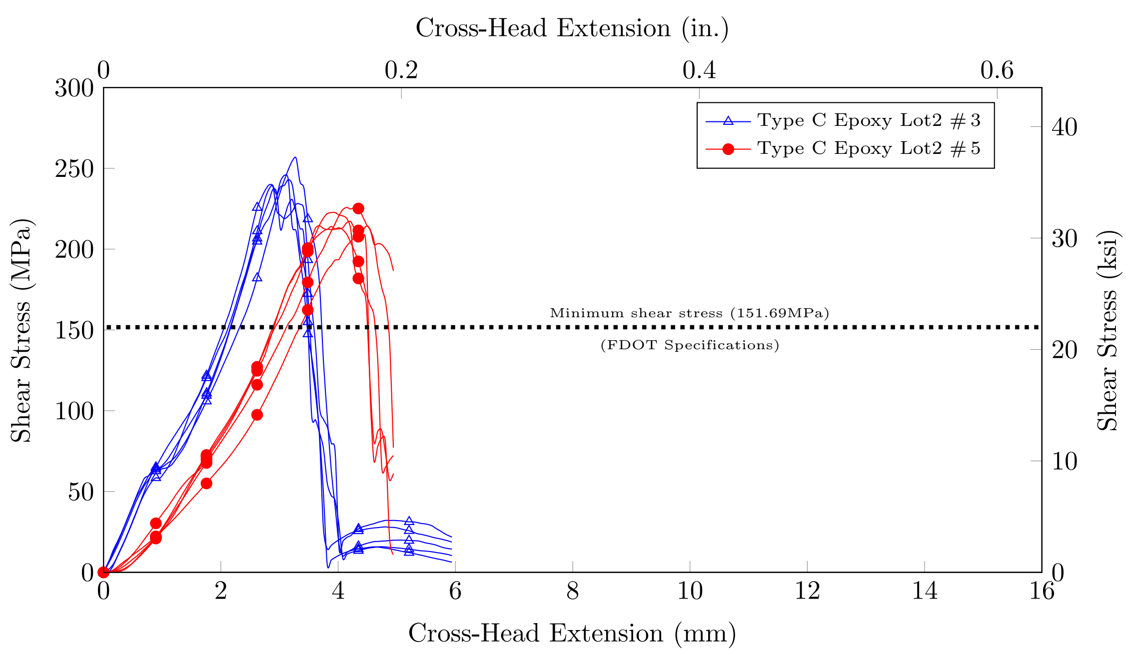

Figure 4.12: Transverse shear stress-extension results of Type C rebar Lot 2 size 3 and 5

4.2 Modes of Failure

To study the failure process, the failed BFRP rebars were analyzed in detail to observe the failure pattern of outer fibers and inner fibers. Figure 4.13 exemplifies the failure patterns of the tested BFRP specimen in response to the applied transverse shear loads. Figure 4.13 shows that the failure mode for all rebars was

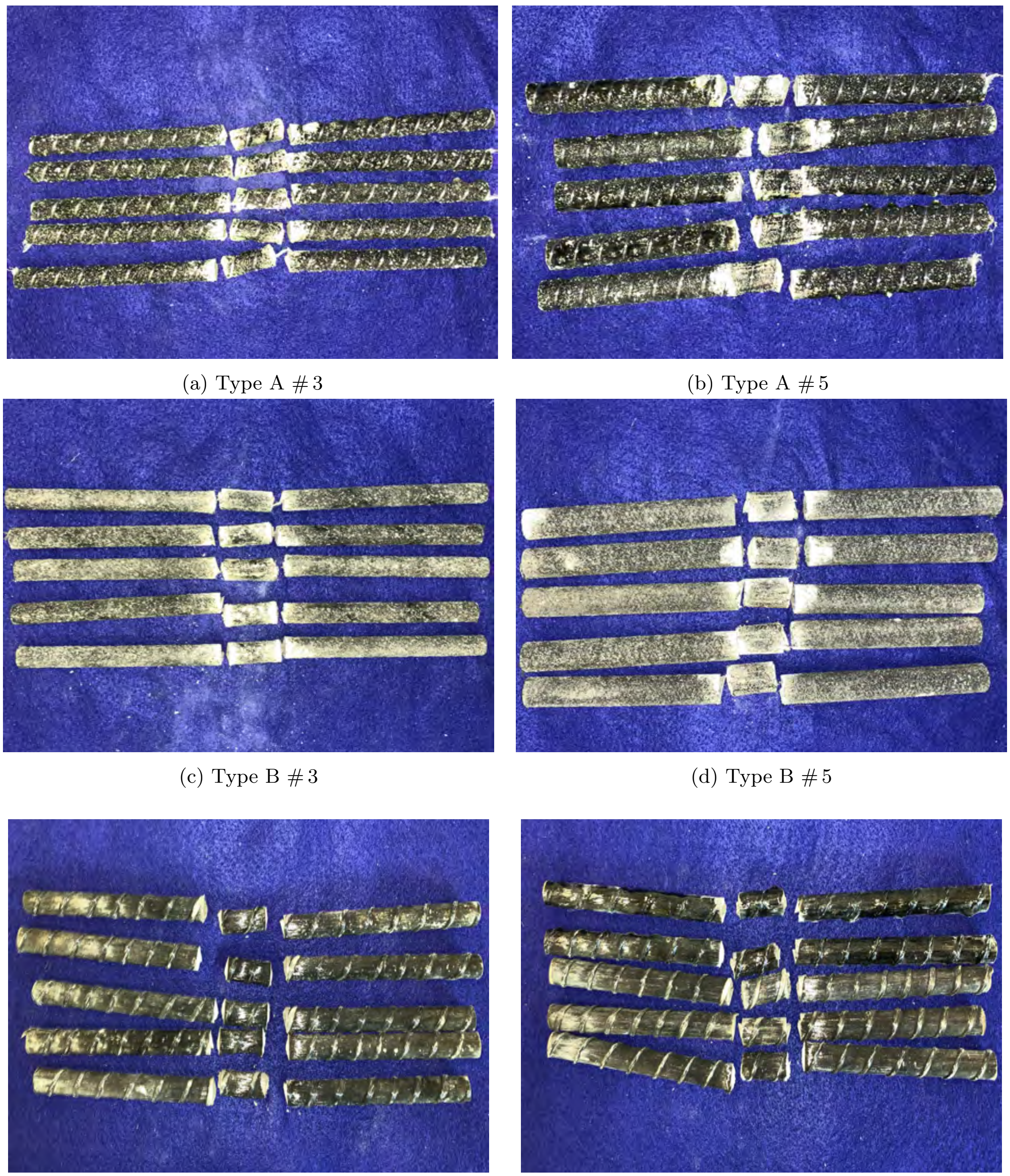

(a) Type A #3 (b) Type A #5

(c) Type B #3 (d) Type B #5

(e) Type C #3 (f) Type C #5

Figure 4.13: Failure pattern for tested rebar after transverse shear test

identical irrespective of the sizes and types.

4.3 Summary of Transverse Shear Properties

The results of the statistical evaluation for the transverse shear strength properties of the tested products are listed in the following Table 4.1. A total of 60 specimen, five for each rebar type, size and lot were tested. The average and all other statistical values were calculated based on a sample size of five specimen, and the corresponding results are shown in the table. For numerical comparison and concluding values, Table 4.1 lists the minimum shear stress ($\wedge$), the maximum shear stress ($\vee$), the average shear stress (μ), the standard deviation (σ), and the coefficient of variation (CV) for each individual test sample.

Table 4.1: Transverse Shear test statistical values for each sample group (US Customary Units)

Sample Group				Statistical Values				
				Shear Stress				
Manuf. Type	Resin Type	Size #	Lot No.	$\wedge$ ksi	$\vee$ ksi	μ ksi	σ ksi	CV %
Rebar A	Epoxy	3	1	25.8	40.4	32.0	5.9	18.51
Rebar A	Epoxy	5	1	15.3	34.3	29.3	8.1	27.62
Rebar B	Vinyl-ester	3	1	36.7	40.3	38.1	1.5	3.89
Rebar B	Vinyl-ester	5	1	30.8	32.9	31.7	0.8	2.62
Rebar C	Epoxy	3	1	28.5	37.3	33.6	3.5	10.30
Rebar C	Epoxy	5	1	34.9	37.5	35.8	1.1	3.01
Rebar A	Epoxy	3	2	29.4	38.3	32.5	3.6	10.94
Rebar A	Epoxy	5	2	26.7	33.1	29.7	2.5	8.58
Rebar B	Vinyl-ester	3	2	37.0	45.5	41.0	3.6	8.72
Rebar B	Vinyl-ester	5	2	30.8	34.7	32.2	1.5	4.73
Rebar C	Epoxy	3	2	28.6	31.5	30.5	1.3	4.29
Rebar C	Epoxy	5	2	31.0	32.8	31.8	0.8	2.40

4.4 Apparent Horizontal Shear Test

The FRP rebar products were tested for horizontal shear properties. The horizontal shear test was conducted according to the ASTM D 4475 (ASTM-International, 2012a) standards.

4.4.1 Load-Displacement

The graphs in Figures 4.14, 4.15, 4.16, 4.17, 4.18, and 4.19 plot the load-displacement behavior of short span 3 point bending. Each rebar type is shown individually—and every specimen within the relevant sample is displayed—to compare # 3 and # 5 from the same type. The x-axis of the graph represents the cross-head frame displacement, and the y-axis represents the applied load.

The graph in Figure 4.14 shows a nearly linear behavior until it reached the ultimate failure load. Following the peak load, a descending branch proceeds with individual local peaks and drops. The peaks and drops represent individual layers of fibers engaged and failing in tension located in the lower part of the specimen experiencing pure tension, while the upper part is in compression. Extension-Horizontal shear behavior of rebar Type B can be seen in the graph in Figure 4.15. Similar to Type A, # 5 Type B rebar sustained

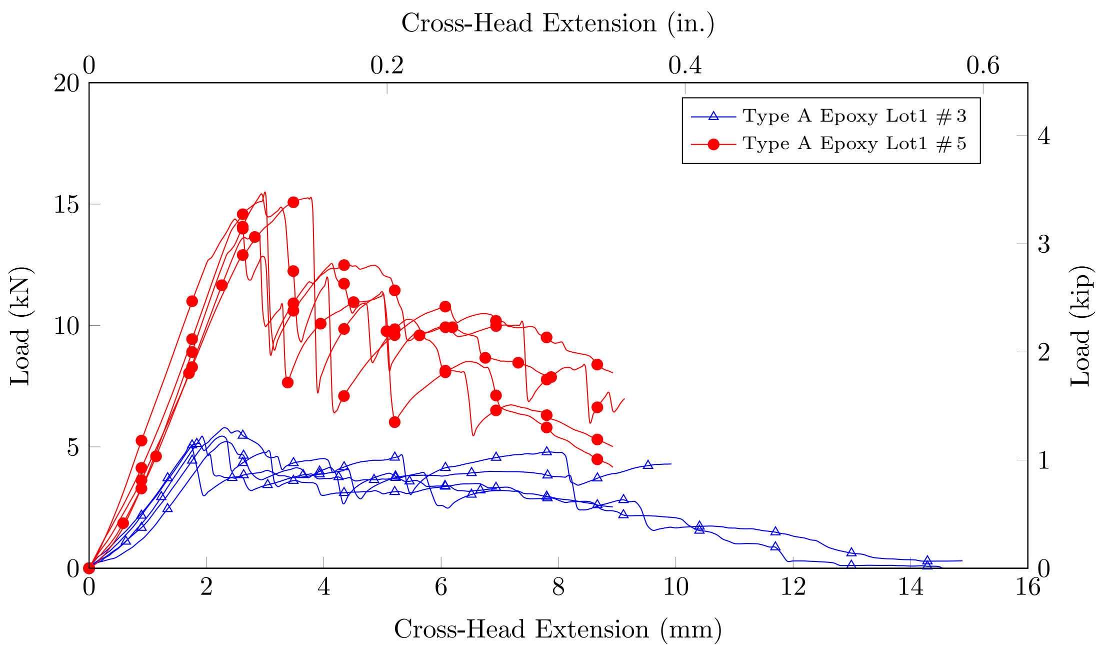

Figure 4.14: Extension-horizontal shear load behavior of rebar Type A Lot 1 size 3 and 5

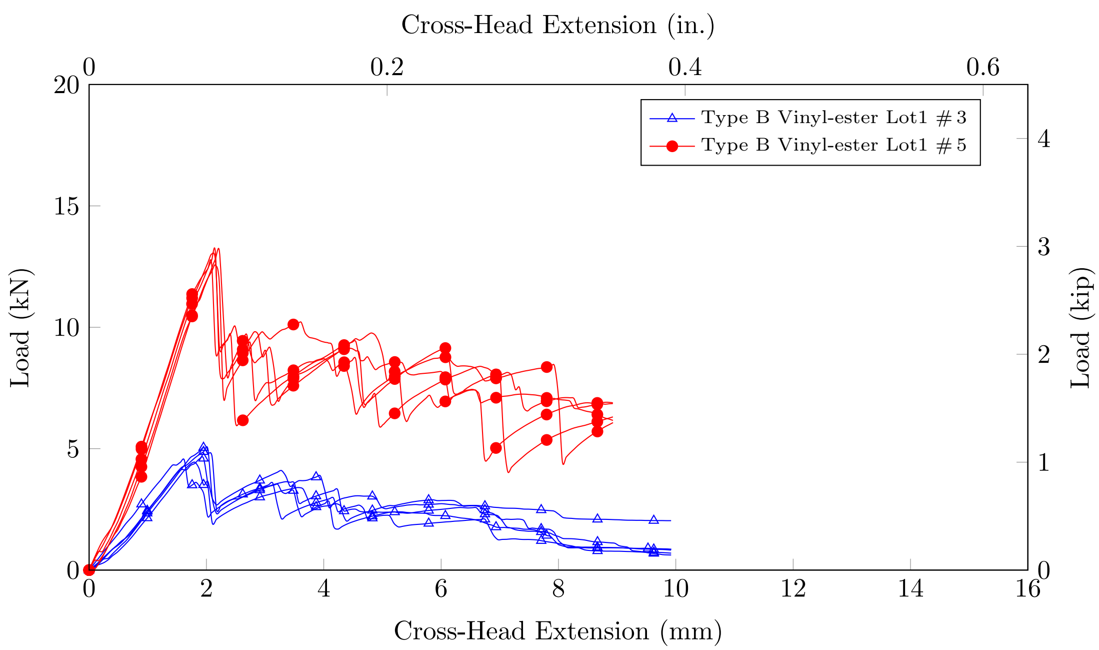

Figure 4.15: Extension-horizontal shear load behavior of rebar Type B Lot 1 size 3 and 5

more load in comparison with # 3 rebars. The failure pattern of # 3 and # 5 Type B rebars was similar and identical to Type A rebar failure pattern. The load - displacement graph of Type C rebar in Figure 4.16 shows a nearly linear behavior until it reached the ultimate failure load. Following the peak load, a descending branch proceeds with individual local peaks and drops. The peaks and drops represent individual layers of fibers engaged and failing in tension located in the lower part of the specimen experiencing pure tension, while the upper part is in compression. The graphs shown in Figures 4.17, 4.18, and 4.19 show the load-displacement behavior of Lot 2 Type A, Type B, and Type C rebars. The graphs show a linear behavior

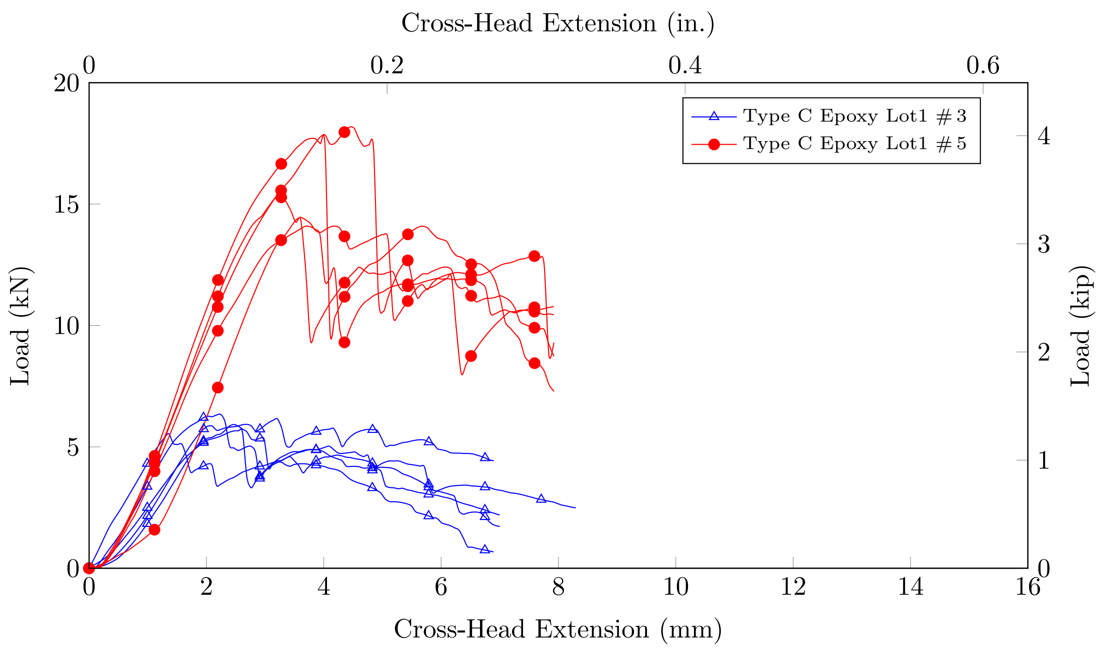

Figure 4.16: Extension-horizontal shear load behavior of Type C rebar Lot 1 size 3 and 5

until it reached approximately 90 % of the ultimate failure load. It can be seen in Figures 4.17 and 4.18

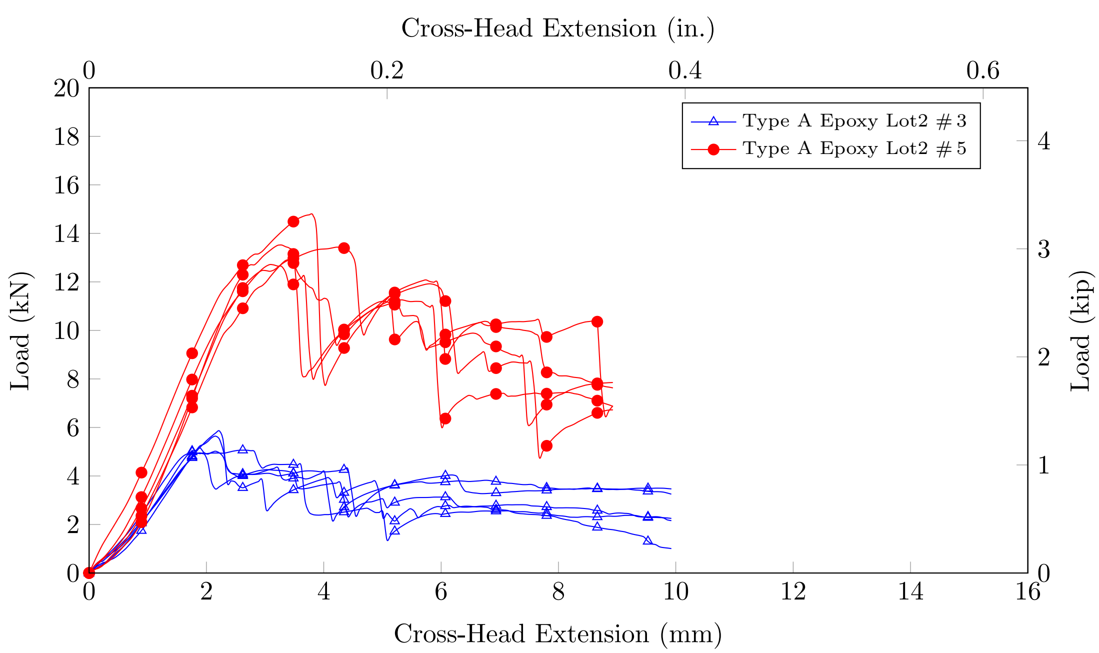

Figure 4.17: Extension-horizontal shear load behavior of rebar Type A Lot 2 size 3 and 5

that the failure behavior of Type A and Type B rebars is identical irrespective of production lot and rebar size. Extension-Horizontal shear behavior of Lot 2 Type C rebars can be seen in the graph in Figure 4.19. Similar to Lot 1, # 5 Lot 2 rebars sustained more load in comparison with # 3 rebars. The failure pattern of # 3 and # 5 Lot 2 rebars was similar and identical to the failure pattern of rebars from Lot 1.

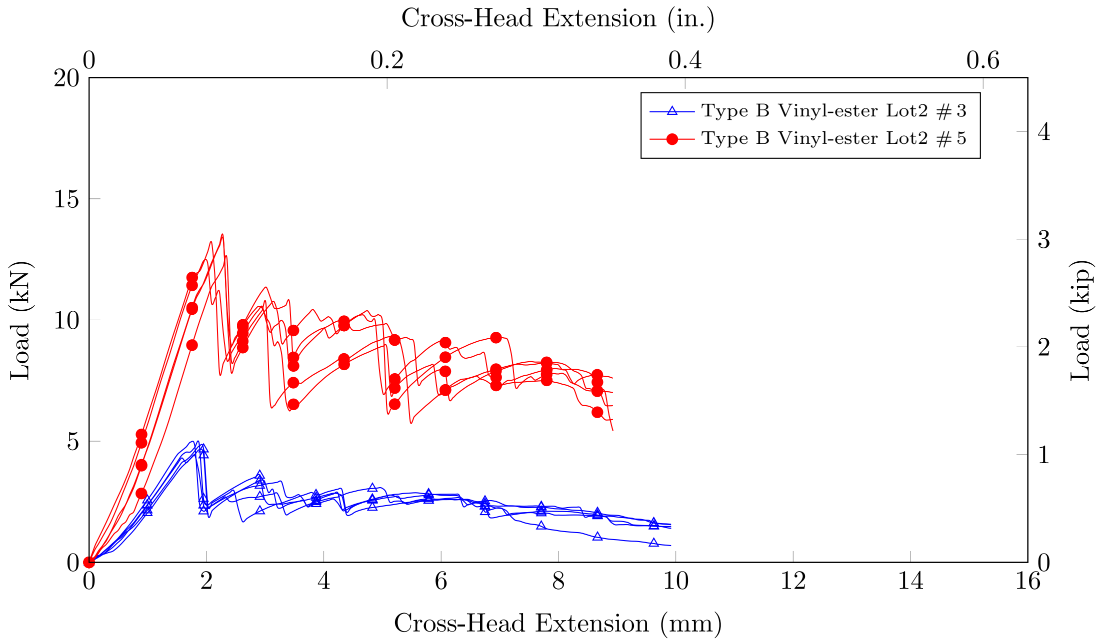

Figure 4.18: Extension-horizontal shear load behavior of rebar Type B Lot 2 size 3 and 5

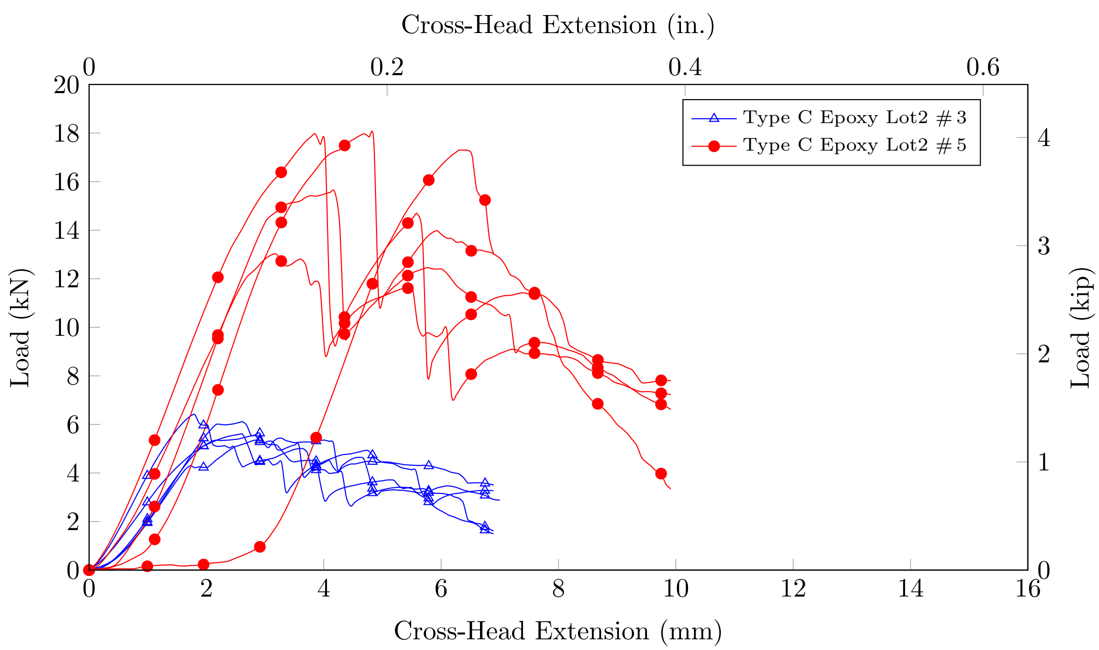

Figure 4.19: Extension-horizontal shear load behavior of Type C rebar Lot 2 size 3 and 5

4.4.2 Stress-Displacement

To provide clarity and to compare the horizontal shear strength performance of the two rebar sizes, stress-strain behavior of rebar is shown in this section via graphs. The following graphs in Figures 4.20, 4.21, 4.22, 4.23, 4.24, and 4.25 show the comparison of the stress - cross-head behavior for the tested BFRP rebars. The x-axis of graph represents the cross-head extension, while the y-axis signifies the measured shear stresses. As expected, a significant difference in peak load between rebar sizes of Type A rebar was observed.

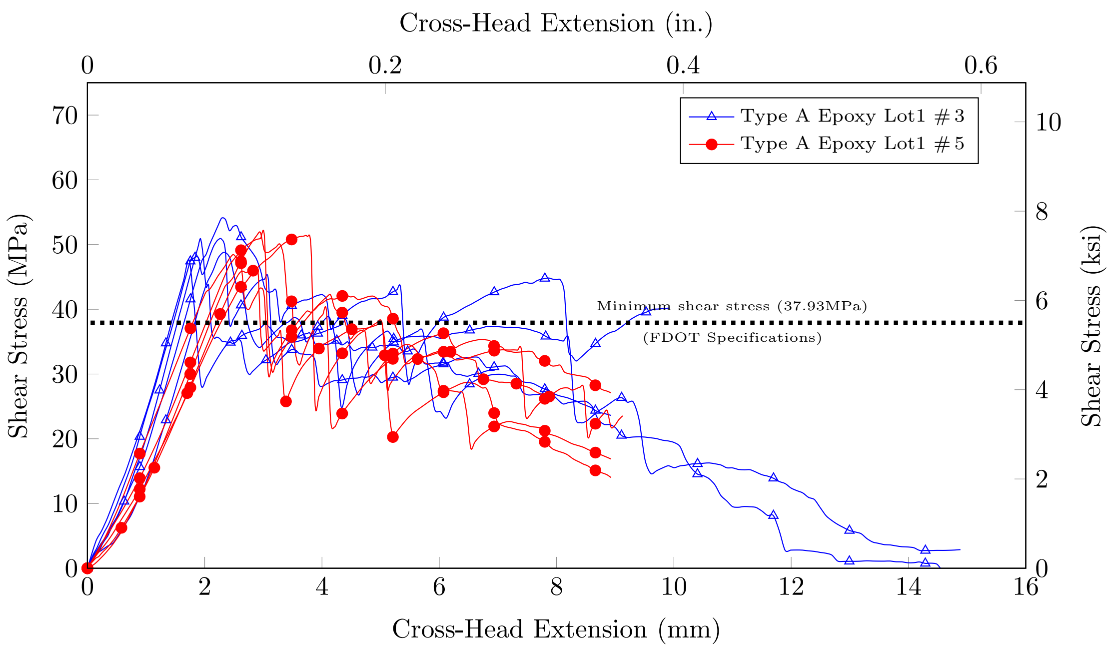

Figure 4.20: Horizontal shear stress vs. extension behavior of rebar Type A Lot 1 size 3 and 5

Nevertheless, the resultant horizontal shear stress is approximately the same regardless of the rebar size. The

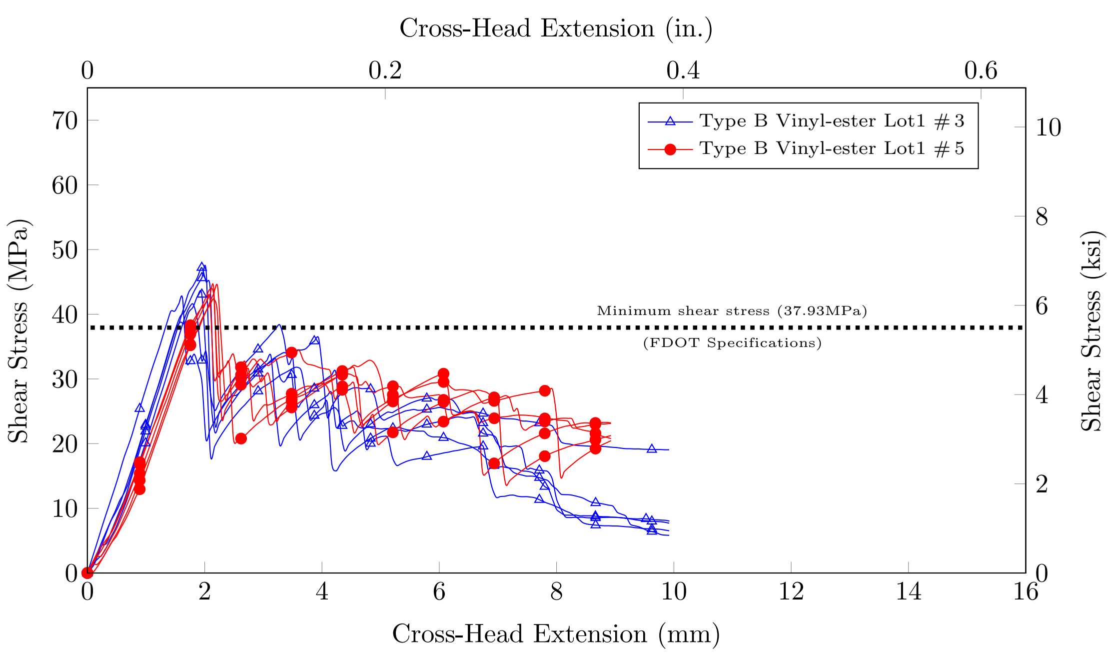

Figure 4.21: Horizontal shear stress vs. extension behavior of rebar Type B Lot 1 size 3 and 5

stress-displacement behavior of rebar Type B shows that the failure pattern was identical for both the sizes but # 5 rebars sustained more stress in comparison to # 3 rebars. As expected, a significant difference in peak load between rebar sizes of Type C Lot 1 rebar was observed. Nevertheless, the resultant horizontal shear stress is approximately the same regardless of the rebar size. The graphs in Figures 4.23, 4.24, and 4.25 are used to compare the stress-displacement behavior of horizontal shear test of # 3 and # 5 rebars from

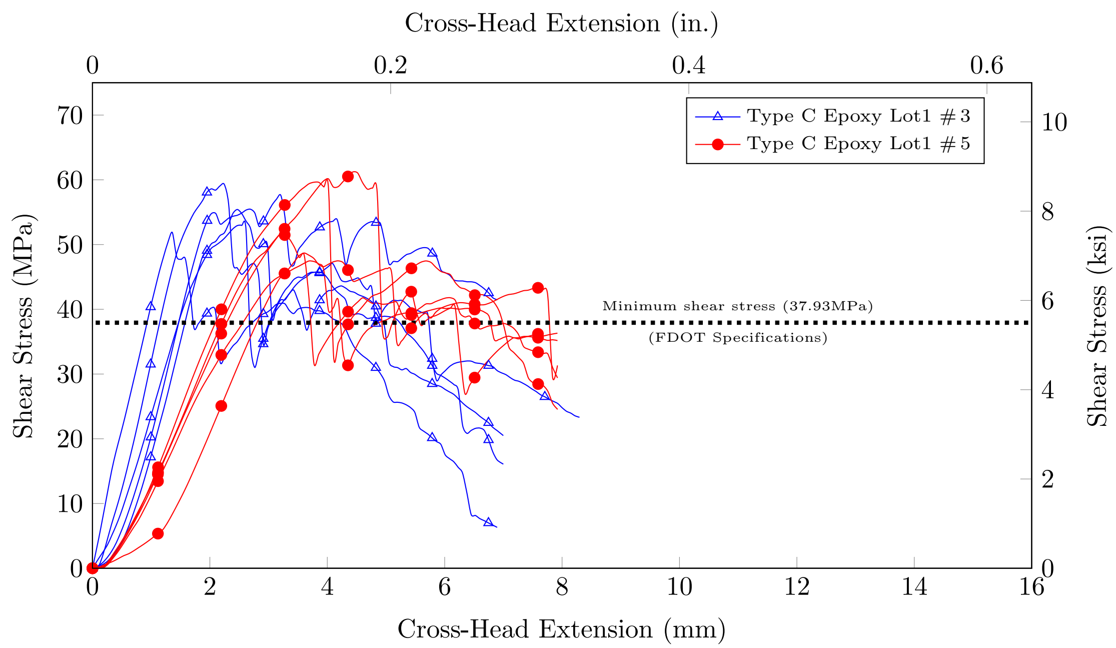

Figure 4.22: Horizontal shear stress-extension behavior of Type C rebar Lot 1 size 3 and 5

Type A, Type B, and Type C from Lot 2. The stress-strain behavior of rebars from Lot 2 show that the

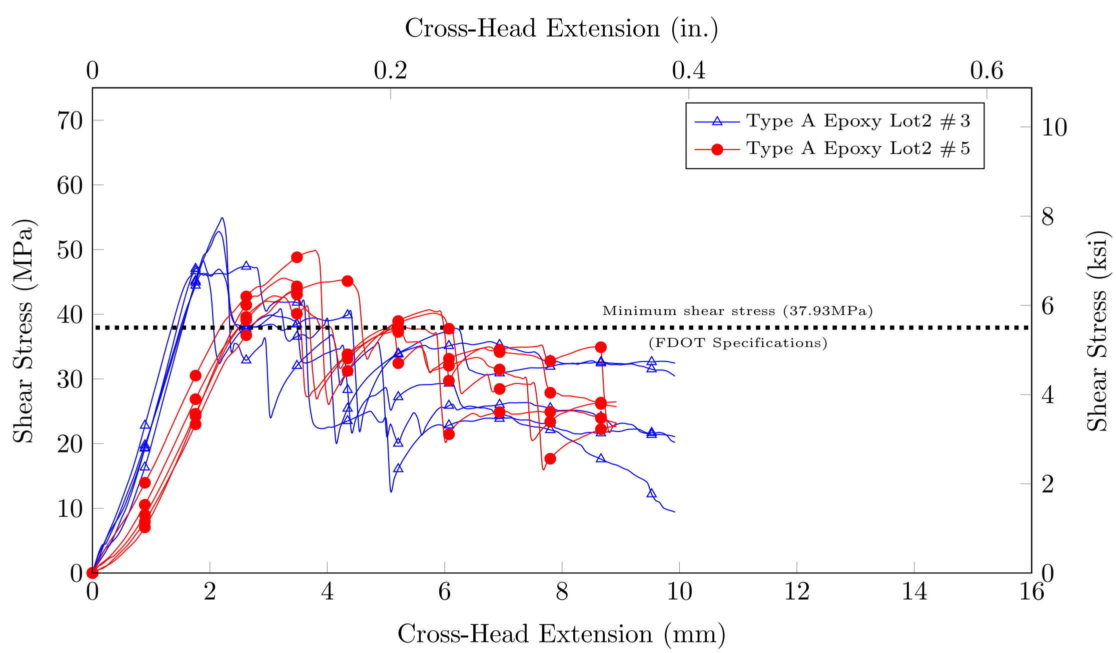

Figure 4.23: Horizontal shear stress vs. extension behavior of rebar Type A Lot 2 size 3 and 5

failure pattern was identical for both the sizes but #5 rebars sustained more stress in comparison to #3 rebars. Figures 4.23 and 4.24 show that all the rebars of Type A and Type B underwent similar stress and strain irrespective of lot and size.

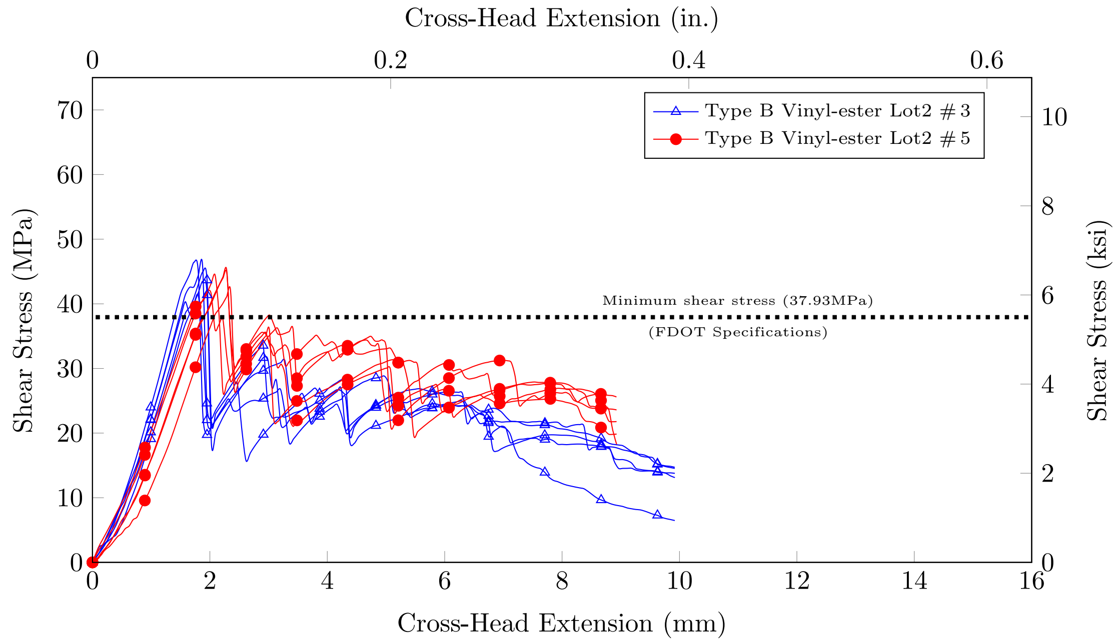

Figure 4.24: Horizontal shear stress vs. extension behavior of rebar Type B Lot 2 size 3 and 5

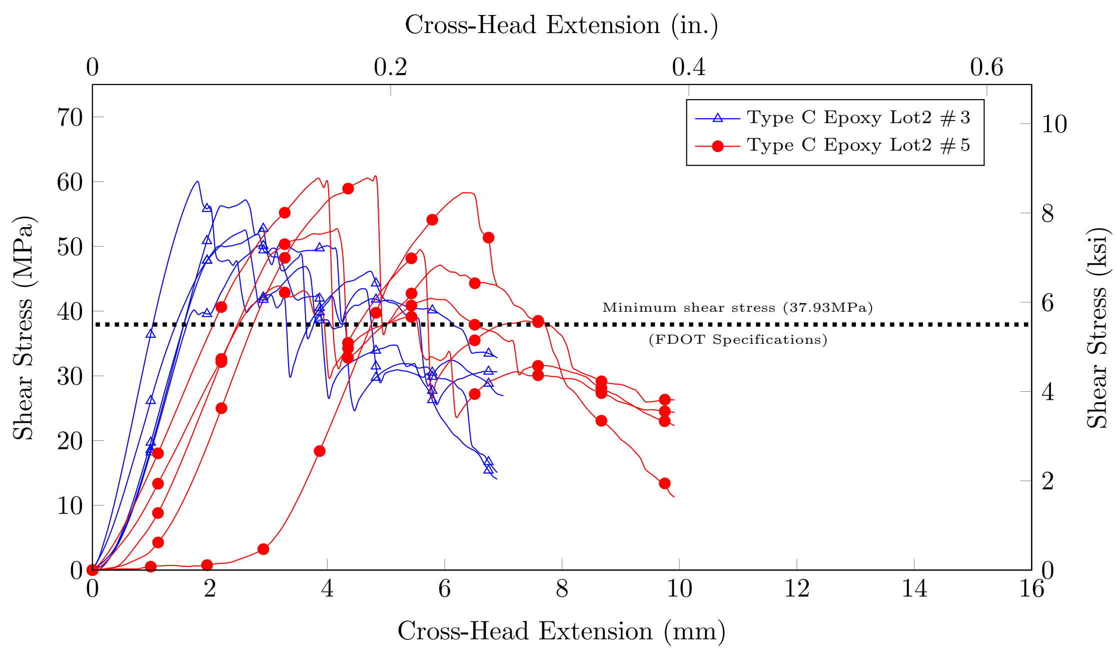

Figure 4.25: Horizontal shear stress-extension behavior of Type C rebar Lot 2 size 3 and 5

4.5 Modes of Failure

To study the failure pattern of BFRP rebars, failure modes of the tested rebars were analyzed. Figure 4.26 shows the failed BFRP specimen after completion of the horizontal shear test. All tested specimens failed due to the apparent horizontal shear force, resulting in horizontal failure planes as observed from the perpendicular cracks to the applied load, through the depth of the cross section. After the peak load, secondary cracks were generated representing the horizontal shear failure plane as each inter-laminar layer of fibers is engaged

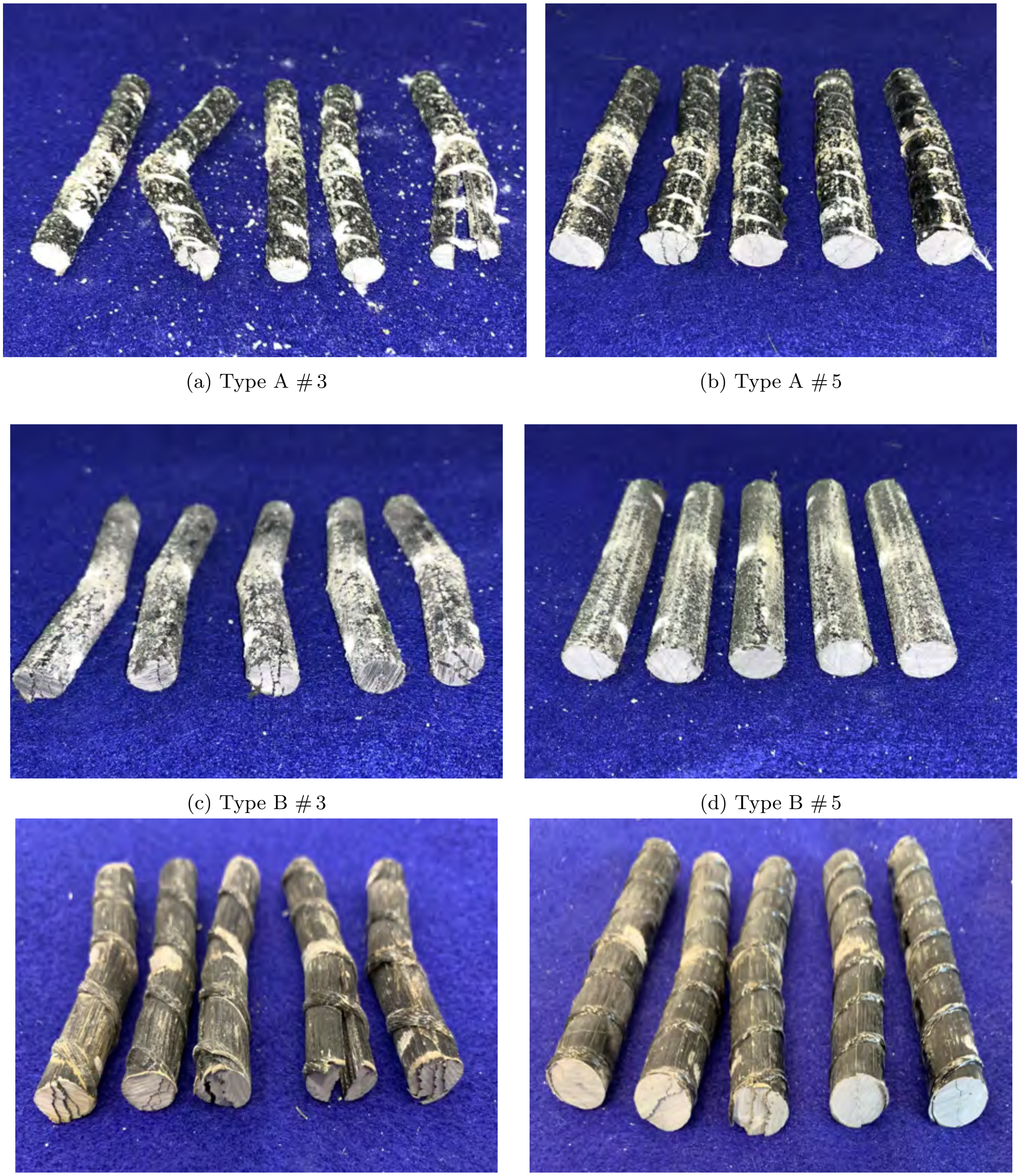

(a) Type A #3 (b) Type A #5

(c) Type B #3 (d) Type B #5

(e) Type C #3 (f) Type C #5

Figure 4.26: Failure pattern for tested rebar after horizontal shear test

in tension and then failing in fiber-matrix interface.

4.6 Summary of Horizontal Shear Strength Properties

The statistical values for the horizontal shear strength properties of the tested products are listed in the following Table 4.2. A total of 60 specimens, five for each type, each size and lot were tested in total. The average of five specimens was assigned to each sample (specimen group) as shown in the table.

Table 4.2: Horizontal Shear test statistical values for each sample group (US Customary Units)

Sample Group				Statistical Values				
				Shear Stress				
Manuf. Type	Resin Type	Size #	Lot No.	$\wedge$ ksi	$\vee$ ksi	μ ksi	σ ksi	CV %
Rebar A	Epoxy	3	1	7.3	8.0	7.5	0.3	3.91
Rebar A	Epoxy	5	1	6.7	7.5	7.2	0.4	5.10
Rebar B	Vinyl-ester	3	1	6.1	6.9	6.5	0.4	5.82
Rebar B	Vinyl-ester	5	1	6.2	6.5	6.4	0.2	2.51
Rebar C	Epoxy	3	1	7.6	8.6	8.1	0.4	5.45
Rebar C	Epoxy	5	1	7.3	8.7	7.9	0.6	7.71
Rebar A	Epoxy	3	2	6.8	8.0	7.3	0.5	7.34
Rebar A	Epoxy	5	2	6.2	7.2	6.6	0.4	5.91
Rebar B	Vinyl-ester	3	2	6.0	6.9	6.6	0.4	5.61
Rebar B	Vinyl-ester	5	2	6.2	6.6	6.4	0.2	3.47
Rebar C	Epoxy	3	2	6.9	8.9	7.8	0.9	11.79
Rebar C	Epoxy	5	2	6.4	8.8	8.0	1.0	12.92

For numerical comparison and concluding values, Table 4.2 lists the minimum shear stress ($\wedge$), the maximum shear stress ($\vee$), the average shear stress (μ), the standard deviation (σ), and the coefficient of variation (CV) for each individual test sample.

4.7 Tensile Test

The rebars were tested according to the ASTM D 7205 (ASTM-International, 2015a) to evaluate the tensile properties. The recorded and processed data of the tensile strength test are shown in this section via graphs and table.

4.7.1 Load-Displacement Behavior

To compare the load-displacement behavior of the different rebar samples and specimens, the graphs in Figures 4.27, 4.28, 4.29, 4.30, 4.31, and 4.32 plot the recorded test data. As shown, the x-axis of the graph represents the cross-head extension—which has to be interpreted with care because it includes the elastic deformation of the load frame and the test fixtures—and the y-axis indicates the applied and measured load. Figure 4.33 shows that # 5 rebar Type A sustained higher failure load in comparison with # 3 rebars and the extension of rebar # 5 was almost thrice that of the # 3 rebars extension. Figure 4.34 shows that the extension of # 5 was more than twice in comparison with # 3 rebars and the peak load was much higher. All the rebars failed in similar fashion. The following graph in Figure 4.29 illustrate the test results for the # 3 and # 5 Type C rebars from Lot 1. After comparing Figures 4.30, 4.31, and 4.29 it can be seen that the rebars of the same size from both the lots of all rebar types sustained the same peak load and failed in the same mode. The extension of rebars from lot 2 of both types was similar to rebars from lot 1 for both sizes. The specimens demonstrated a linear characteristic at around 10 kN until the peak load.

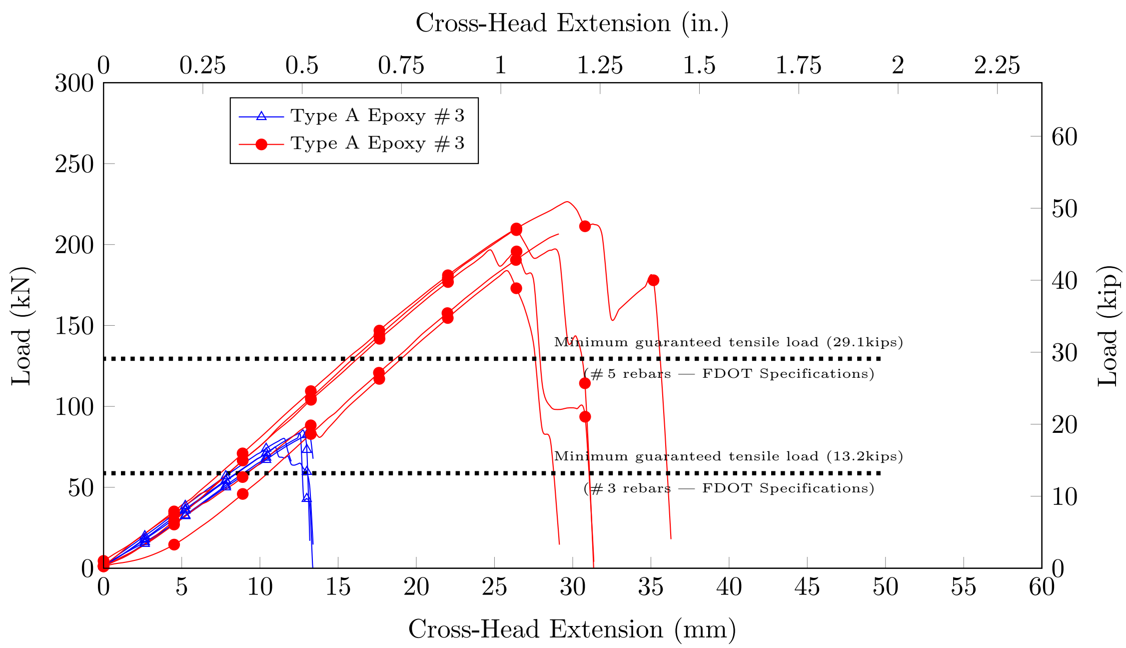

Figure 4.27: Tensile strength-displacement behavior of rebar Type A Lot 1 size 3 and 5

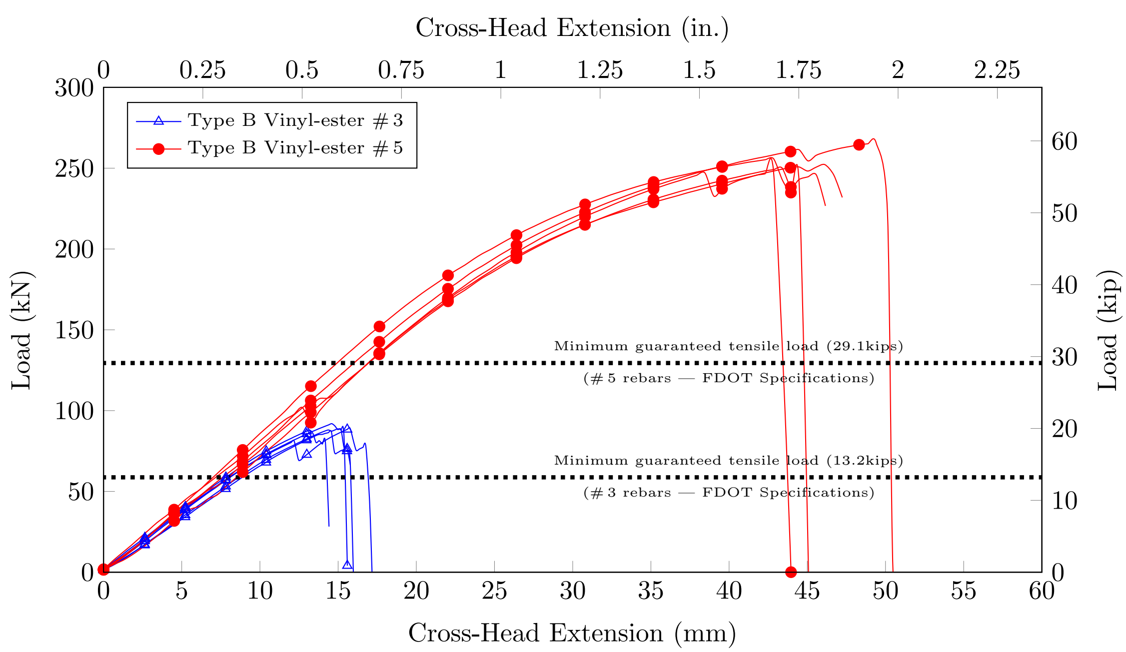

Figure 4.28: Tensile strength-displacement behavior of rebar Type B Lot 1 size 3 and 5

The common behavior after the maximum load was overcome was a stepwise loss of load with little inclines until the next load loss occurred. With increasing cross-head extension in the post-failure region, the load decreased slightly, but then stagnated or even regained some strength throughout further extension, multiple times, until the specimen failed completely. During testing, it was observed that after the maximum load was reached, the rebars delaminated and flared out more and more, as these load-drops occurred (ultimately producing the failure patterns detailed in Section 4.8).

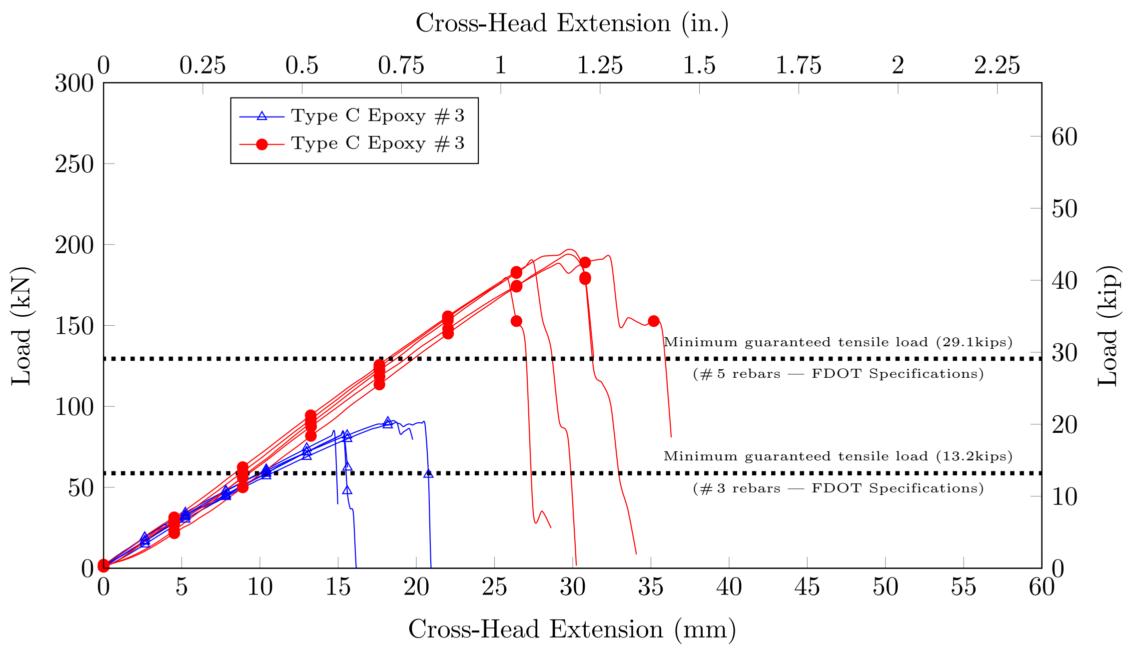

Figure 4.29: Tensile strength-displacement behavior of Basalt Technologies UK Ltd (BASTECH^{TM}) rebar Lot 1 size 3 and 5

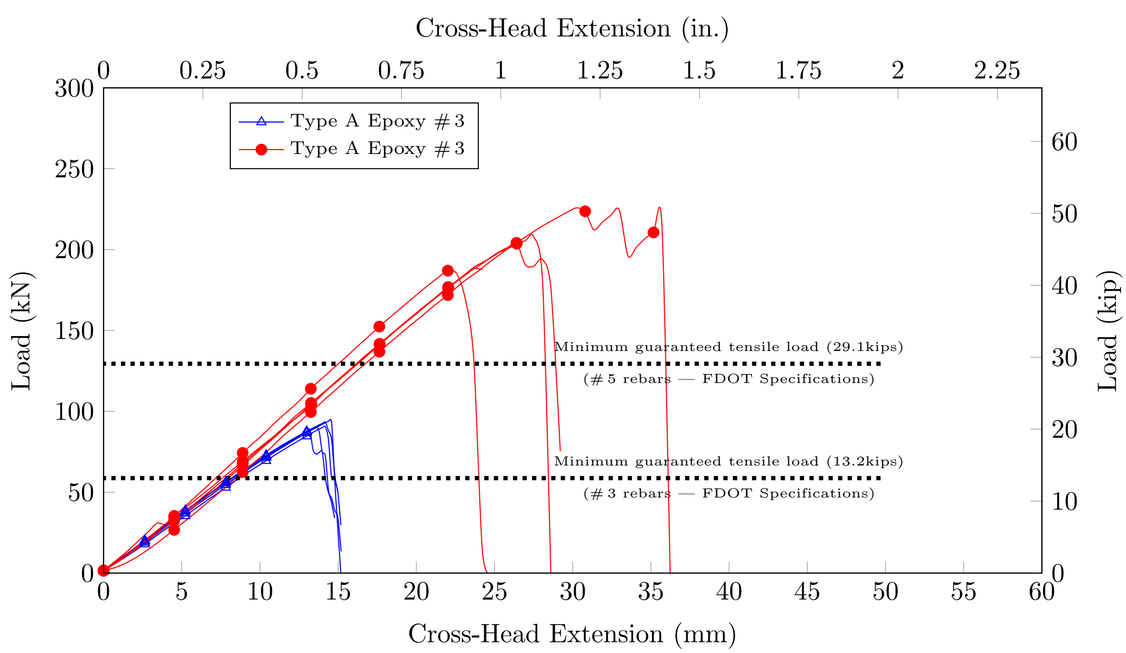

Figure 4.30: Tensile strength-displacement behavior of rebar Type A Lot 2 size 3 and 5

4.7.2 Stress-Strain Behavior

The stress-strain behavior of the failed rebars of all types was plotted to quantify and compare the elastic moduli of the tested BFRP rebars. The data in Figures 4.33, 4.34, 4.35, 4.36, 4.37, and 4.38 were plotted to compare the stress-strain behavior of the different rebar types. Accordingly, the x-axis shows the applied stress while the y-axis represents the outermost surface strain that was measured with an external extensometer.

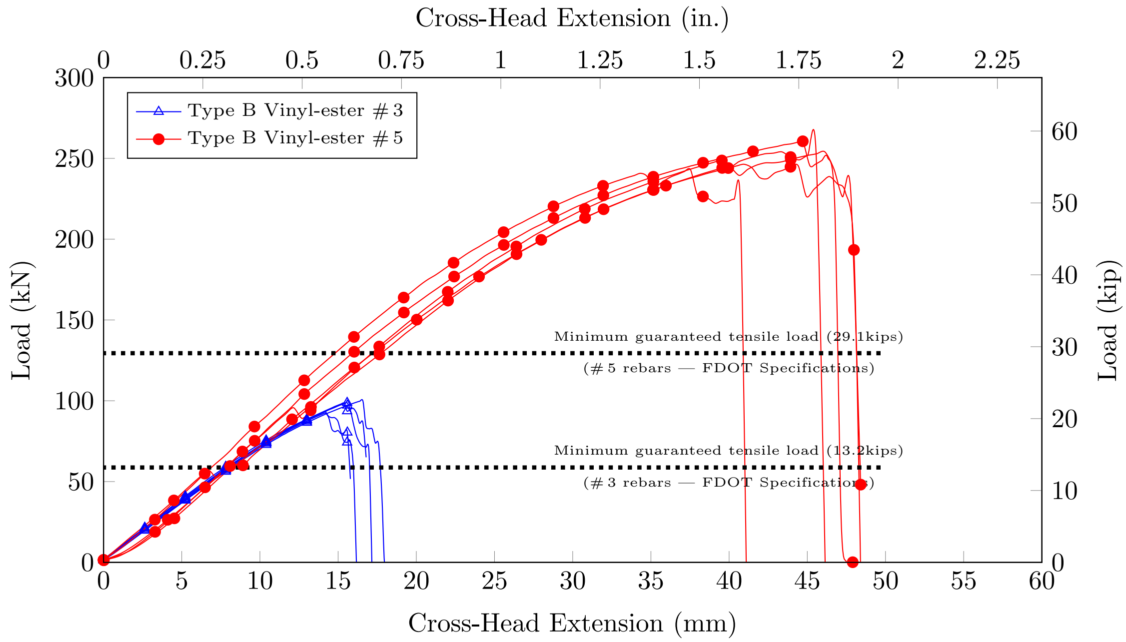

Figure 4.31: Tensile strength-displacement behavior of rebar Type B Lot 2 size 3 and 5

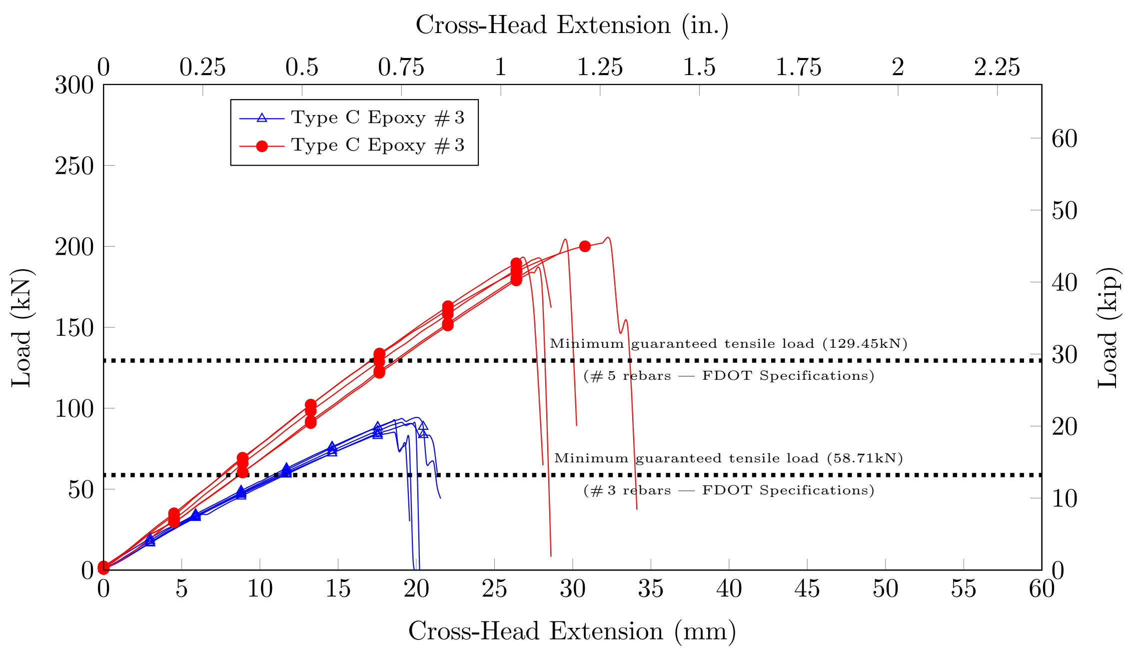

Figure 4.32: Tensile strength-displacement behavior of Basalt Technologies UK Ltd (BASTECH^{TM}) rebar Lot 2 size 3 and 5

The results plotted in the graph in Figure 4.33 show that though the load capacities of the different sized rebars vary widely, the slope of the stress-strain curve was identical for all the rebars. It can be seen in Figure 4.34 that stress-strain behavior of rebar Type B are identical for both the rebar sizes. The stress-strain behavior of rebars from lot 2 as shown in Figures 4.36, 4.37, and 4.38 show that the slopes of bars from Lot 1 and Lot 2 were identical.

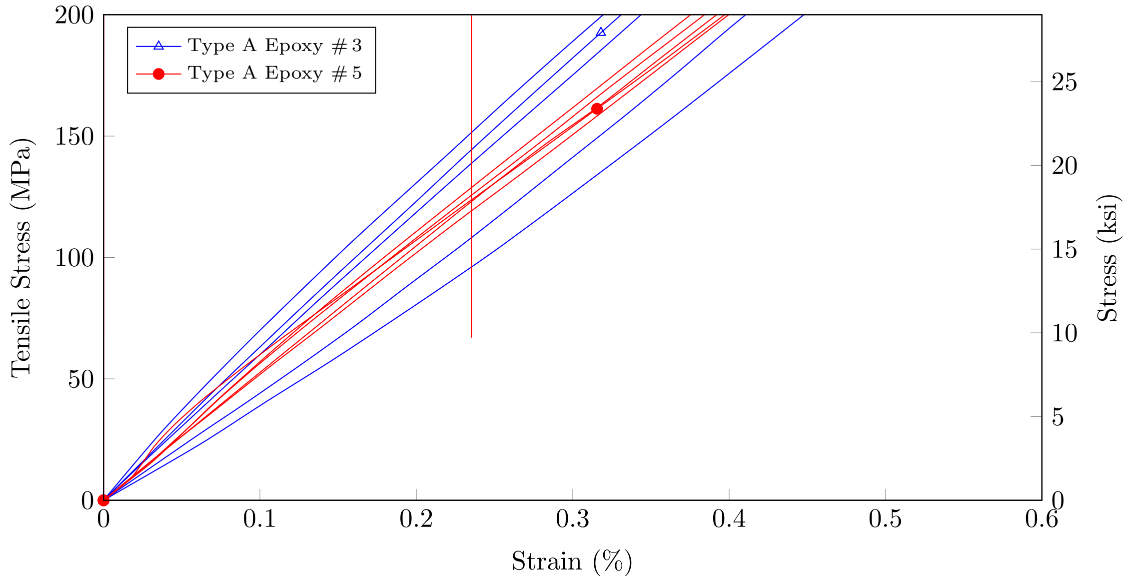

Figure 4.33: Tensile stress-strain behavior of rebar Type A Lot 1 rebar size 3 and 5

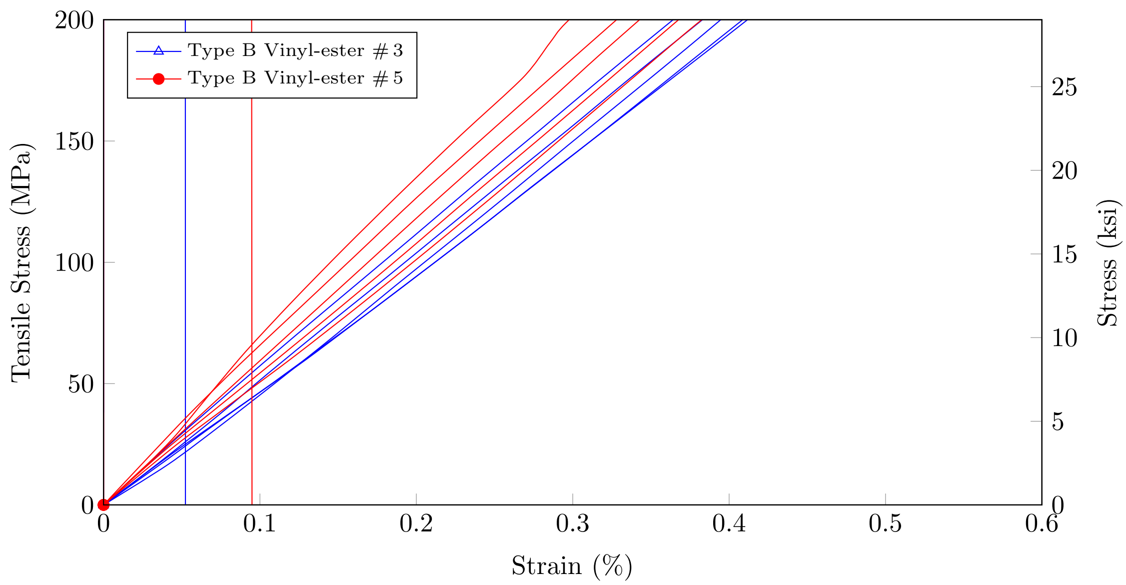

Figure 4.34: Tensile stress-strain behavior of rebar Type B Lot 1 rebar size 3 and 5

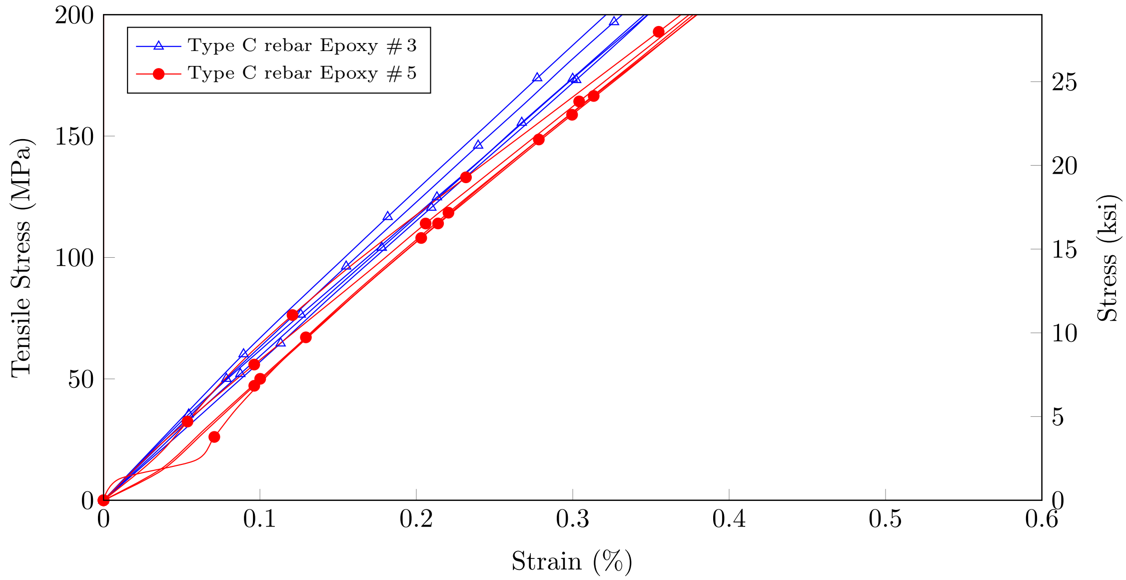

Figure 4.35: Tensile stress-strain behavior of Type C rebar Lot 1 rebar size 3 and 5

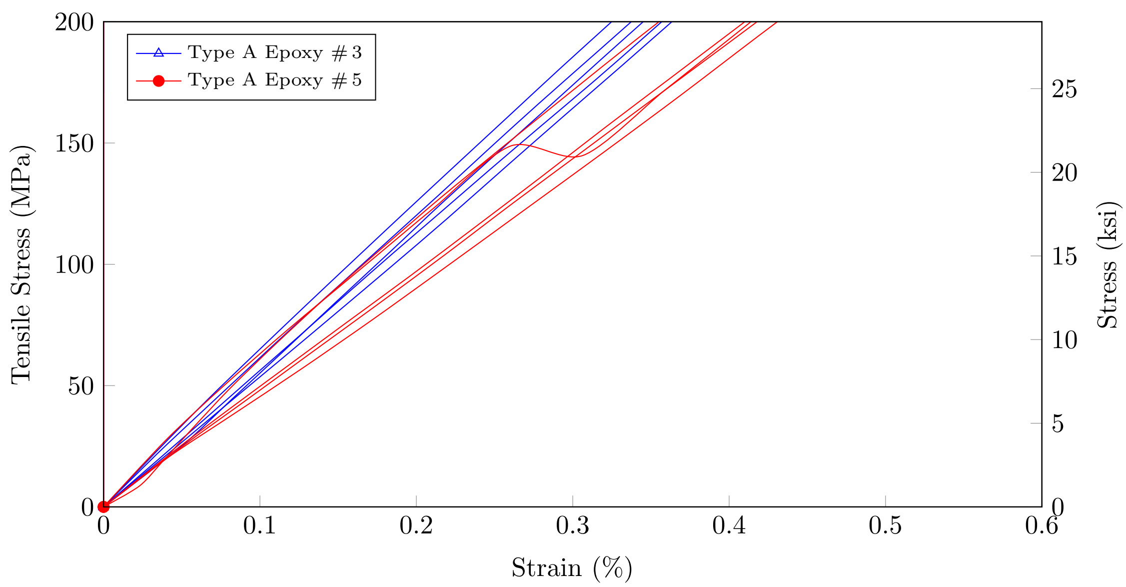

Figure 4.36: Tensile stress-strain behavior of rebar Type A Lot 2 rebar size 3 and 5

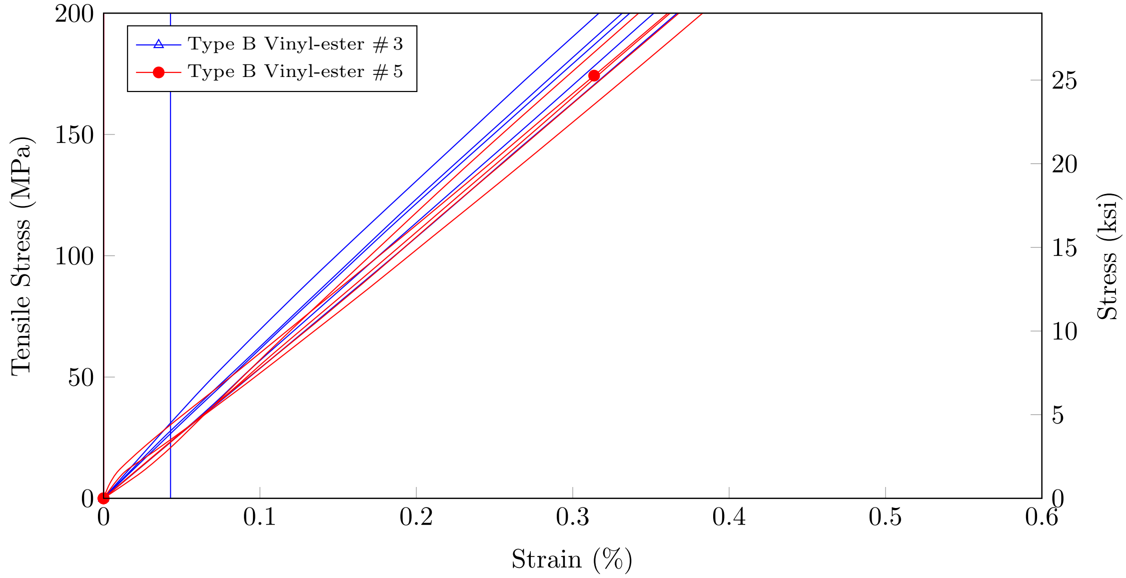

Figure 4.37: Tensile stress-strain behavior of rebar Type B Lot 2 rebar size 3 and 5

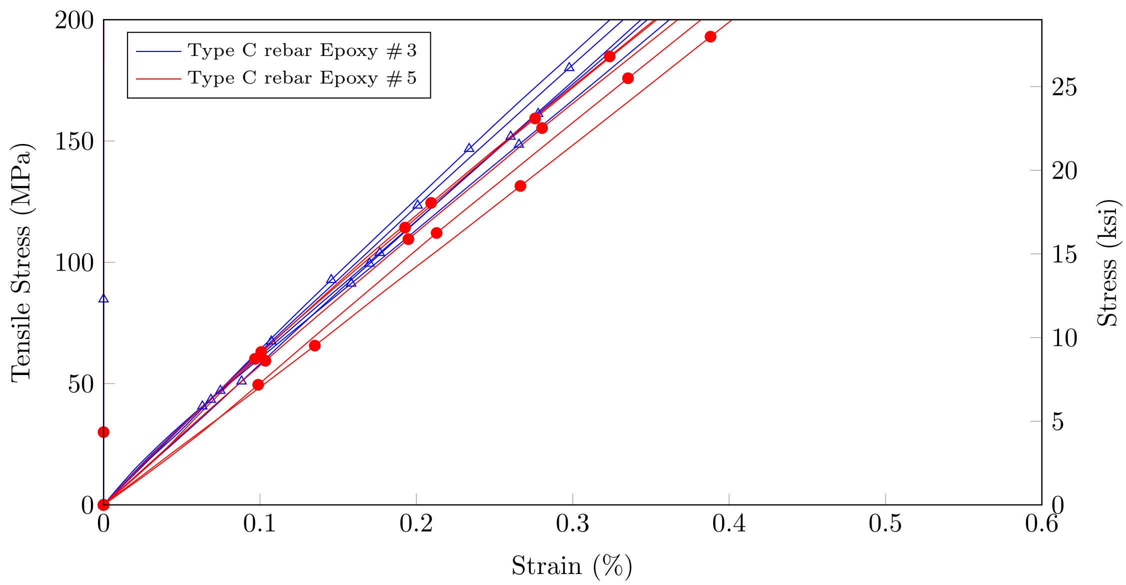

Figure 4.38: Tensile stress-strain behavior of Type C rebar Lot 2 size 3 and 5

4.8 Modes of Failure

According to ASTM D 7205, three different failure modes may occur during a tensile strength test. The first and expected one is the tensile rupture outside of the anchor pipes. Due to insufficient sample preparation or test procedure issues, two more failure modes may occur. The rebar could slip within the grouted anchor (rebar slippage) or the anchor could slip out of the fixture/grips (anchor slippage). Therefore, the last two described failure modes lead to unusable results when defining the material characteristics. However, for this research project, no specimen failed due to rebar or anchor slippage. Hence, tensile rupture of the BFRP rebar was the recorded failure mode for each bar that was tested.

Figure 4.39a and 4.40a show the failed specimens of Type A rebars. It can be seen that all specimens, regardless of their diameter, displayed similar failure pattern. The fibers formed a brush type of failure and all specimens suffered fiber delamination throughout the entire free specimen length. Figure 4.39b and 4.40b present the post failure pattern of Type B rebar specimens. It is shown that all the rebar sizes had an identical failure. The fibers were delaminated and a distinct brush-like failure was observed. Figure 4.39c and 4.40c show the failed specimens of # 3 and # 5 Type C rebars. All the specimens failed in a similar manner. After the peak load was reached, an abrupt brittle failure of the rebar was observed close to the anchor.

(a) Type A

(b) Type B

(c) Type C

Figure 4.39: # 3 rebar final failure pattern after tensile test

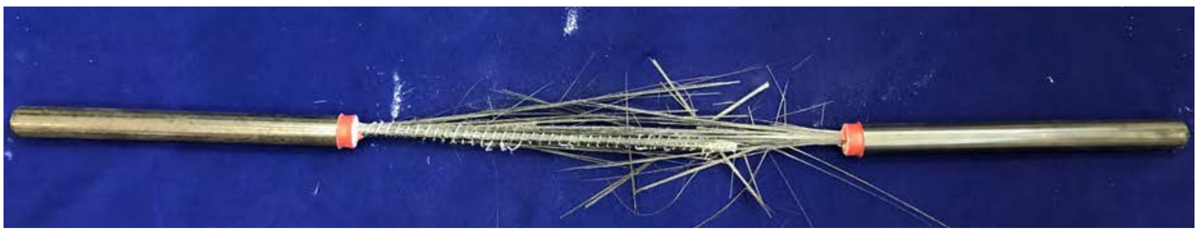

(a) Type A

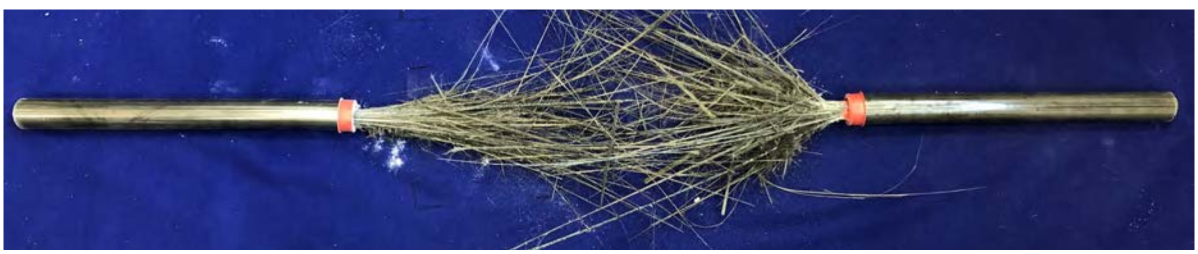

(b) Type B

(c) Type C

Figure 4.40: # 5 rebar final failure pattern after tensile test

4.9 Summary of Tensile Properties

The results of the statistical evaluation for the measured tensile properties of all products along with the elastic modulus property are listed in the following Table 4.3. A total of 60 specimen, 5 per rebar size, type and lot, were tested and analyzed to determine the results shown in the table. For numerical comparison and concluding values, Table 4.3 lists the minimum tensile stress ($\wedge$), the maximum tensile stress ($\vee$), the average tensile stress (μ), the standard deviation (σ), and the coefficient of variation (CV) for each individual test sample.

Table 4.3: Tensile strength test statistical values for each sample group (US Customary Units)

Sample group				Statistical values									
				Tensile Strength					Elastic Modulus				
Manf. Type	Resin Type	Size #	Lot No.	$\wedge$ ksi	$\vee$ ksi	μ ksi	σ ksi	CoV %	$\wedge$ ksi	$\vee$ ksi	μ ksi	σ ksi	CoV %
Rebar A	Epoxy	3	1	149.3	170.9	162.3	8.2	5.05	6358	8638	7788	1030	13.21
Rebar A	Epoxy	5	1	134.1	162.8	149.1	10.7	7.20	6825	7575	7241	277	3.81
Rebar A	Epoxy	3	2	178.7	188.9	183.5	4.3	2.37	8011	11 460	8958	1430	15.96
Rebar A	Epoxy	5	2	137.9	166.5	148.9	11.7	7.87	5352	8036	6780	961	14.17
Rebar B	Vinly-ester	3	1	174.5	184.9	178.3	3.9	2.18	7050	7888	7441	364	4.89
Rebar B	Vinly-ester	5	1	180.1	194.0	185.6	5.1	2.75	7563	9134	8319	615	7.39
Rebar B	Vinly-ester	3	2	186.1	200.1	193.7	6.7	3.48	7938	8796	8425	348	4.13
Rebar B	Vinly-ester	5	2	177.6	190.1	183.8	4.9	2.68	7513	8619	7955	412	5.18
Rebar C	Epoxy	3	1	1149	1259	1192	56.2	4.71	56	60	58	2	3.05
Rebar C	Epoxy	5	1	905	987	958	32.4	3.37	51	56	54	2	4.06
Rebar C	Epoxy	3	2	1183	1310	1259	46.9	3.72	53	61	58	3	5.21
Rebar C	Epoxy	5	2	923	1019	975	35.8	3.67	50	55	54	2	3.86

References

ASTM (2014). *Standard Test Method for Moisture Absorption Properties and Equilibrium Conditioning of Polymer Matrix Composite Materials*, (D5229). ASTM International, West Conshohocken, PA.

ASTM-International (2011). *Standard Test Method for Ignition Loss of Cured Reinforced Resins*, (D2584-11). West Conshohocken, PA.

ASTM-International (2012a). *Standard Test Method for Apparent Horizontal Shear Strength of Pultruded Reinforced Plastic Rods By the Short-Beam Method*, (D4475 - 02 (REAPPROVED 2008)). West Conshohocken, PA.

ASTM-International (2012b). *Standard Test Method for Transverse Shear Strength of Fiber-reinforced Polymer Matrix Composite Bars*, (D7617/D7617M - 11). West Conshohocken, PA.

ASTM International (2014). *Standard Test Method for Bond Strength of Fiber-Reinforced Polymer Matrix Composite Bars to Concrete by Pullout Testing*, (D7913/D7913M). West Conshohocken, PA.

ASTM-International (2015a). *Standard Test Method for Tensile Properties of Fiber Reinforced Polymer Matrix Composite Bars*, (D7205/D7205M – 06 Reapproved 2011). West Conshohocken, PA.

ASTM-International (2015b). *Standard Test Methods for Density and Specific Gravity (Relative Density) of Plastics by Displacement*, (D792-13). West Conshohocken, PA.

Rice, E. W., Baird, R. B., Eaton, A. D., Clesceri, L. S., et al. (2012). *Standard methods for the examination of water and wastewater*, (Vol. 10). American Public Health Association Washington, DC.